Dendritic glutamate receptor channels in rat hippocampal CA3 and CA1 pyramidal neurons

Nelson Spruston, Peter Jonas and Bert Sakmann

Max-Planck-Institut für medizinische Forschung, Abteilung Zellphysiologie, Jahnstrasse 29, D-69120 Heidelberg, Germany

1. Properties of dendritic glutamate receptor (GluR) channels were investigated using fast application of glutamate to outside-out membrane patches isolated from the apical dendrites of CA3 and CA1 pyramidal neurons in rat hippocampal slices. CA3 patches were formed (15–76 μm from the soma) in the region of mossy fibre (MF) synapses, and CA1 patches (25–174 μm from the soma) in the region of Schaffer collateral (SC) innervation.

2. Dual-component responses consisting of a rapidly rising and decaying component followed by a second, substantially slower, component were elicited by 1 ms pulses of 1 mM glutamate in the presence of 10 μM glycine and absence of external Mg^{2+}. The fast component was selectively blocked by 2–5 μM 6-cyano-7-nitroquinoxaline-2,3-dione (CNQX) and the slow component by 30 μM D-2-amino-5-phosphonopentanoic acid (D-AP5), suggesting that the fast and slow components were mediated by the GluR channels of the L-α-amino-3-hydroxy-5-methyl-4-isoxazolepropionate (AMPA) and NMDA type, respectively. The peak amplitude ratio of the NMDA to AMPA receptor-mediated components varied between 0·03 and 0·62 in patches from both CA3 and CA1 dendrites. Patches lacking either component were rarely observed.

3. The peak current–voltage (I–V) relationship of the fast component was almost linear, whereas the I–V relationship of the slow component showed a region of negative slope in the presence of 1 mM external Mg^{2+}. The reversal potential for both components was close to 0 mV.

4. Kainate-preferring GluR channels did not contribute appreciably to the response to glutamate. The responses to 100 ms pulses of 1 mM glutamate were mimicked by application of 1 mM AMPA, whereas 1 mM kainate produced much smaller, weakly desensitizing currents. This suggests that the fast component is primarily mediated by the action of glutamate on AMPA-preferring receptors.

5. The mean elementary conductance of AMPA receptor channels was about 10 pS, as estimated by non-stationary fluctuation analysis. The permeability of these channels to Ca^{2+} was low ($\sim$5% of the permeability to Cs^+).

6. The elementary conductance of NMDA receptor channels was larger, with a main conductance state of about 45 pS. These channels were 3·6 times more permeable to Ca^{2+} than to Cs^+.

7. AMPA receptor-mediated currents activated rapidly in response to 1 ms pulses of 1 mM glutamate and deactivated with a predominant, fast time constant and a smaller, slower component ($\tau_1 \approx 2$ ms, $\tau_2 \approx 8$ ms, contributing $\sim$80 and $\sim$20% to the total decay amplitude, respectively). Desensitization of the current during a 100 ms pulse was best fitted by two time constants ($\tau_1 \approx 10$ ms, $\sim$60%; $\tau_2 \approx 34$ ms, $\sim$40%).

8. NMDA receptor-mediated currents in response to 1 ms pulses of 1 mM glutamate activated and deactivated much more slowly than AMPA receptor-mediated currents. The time course could be described by a single exponential rising phase ($\tau \approx 7$ ms) followed by a double exponential decay ($\tau_1 \approx 200$ ms, $\sim$80%; $\tau_2 \approx 1$–3 s, $\sim$20%).

9. Mg^{2+} blocked the NMDA component in a voltage-dependent manner, with a half-maximal inhibitory concentration (IC_{50}) of 21 μM at -80 mV. At physiological Mg^{2+} concentrations, block of the NMDA component could be rapidly relieved with voltage jumps from negative to positive potentials. Block of the current upon return to negative potentials occurred almost instantaneously.

10. Zn^{2+} also selectively blocked the NMDA receptor-mediated current with an IC_{50} of 22 μM, but this block differed from that of Mg^{2+} in that it showed little voltage dependence. Rapid application of Zn^{2+} together with glutamate produced partial block of the current. More block was observed if Zn^{2+} and glutamate were co-applied when NMDA receptor channels were already open.

11. The functional properties of dendritic GluRs were similar to those found at the soma. Knowledge of these properties facilitated simulations investigating the contribution of coactivated AMPA and NMDA receptors to synaptic depolarization and Ca^{2+} entry into dendritic spines. Because of its slow deactivation, the NMDA receptor-mediated current contributes substantially to depolarization and Ca^{2+} entry and is susceptible to modulation over a period of seconds, either by backpropagating action potentials or by the release of Zn^{2+} from presynaptic boutons.

Glutamate is the major excitatory neurotransmitter in the central nervous system. At most excitatory synapses, release of glutamate is believed to coactivate two different types of ligand-gated ion channels: AMPA- and NMDA-type GluR channels. There is evidence that both types of receptors are activated at synapses on CA3 and CA1 pyramidal neurons of the hippocampus (Forsythe & Westbrook, 1988; Bekkers & Stevens, 1989; Hestrin, Nicoll, Perkel & Sah, 1990; McBain & Dingeldine, 1992; Jonas, Major & Sakmann, 1993). The functional properties of AMPA and NMDA receptor channels have also been studied extensively in somatic membrane patches isolated from hippocampal neurons in culture (Jahr & Stevens, 1987; Lester, Clements, Westbrook & Jahr, 1990; Patneau, Vyklicky & Mayer 1993) and in brain slices (Colquhoun, Jonas & Sakmann, 1992). Relatively little is known, however, about the functional properties of GluR channels in the postsynaptic membrane. It is important that this issue is addressed, especially in view of the fact that studies on recombinant AMPA and NMDA receptor channels have shown that a plethora of different channel properties can be obtained through expression of different subunit combinations, alternative mRNA splicing, and post-transcriptional mRNA editing (Burnashev, 1993; Wisden & Seeburg, 1993). It is also important because these channels are thought to be important for the induction of long-term changes in synaptic strength (Bliss & Collingridge, 1993).

Much of what is known about the properties of subsynaptic GluR channels comes from studies of excitatory postsynaptic currents (EPSCs). Such studies offer the advantage of activating synaptic channels in a physiological way, but suffer from problems associated with inadequate voltage and space clamp (Spruston, Jaffe, Williams & Johnston, 1993) and limited resolution due to the noise in whole-cell recordings. These problems can be avoided by mimicking

synaptic release using fast application of glutamate to outside-out membrane patches. This method provides the added advantage of allowing the transmitter to be applied under controlled conditions that facilitate kinetic analysis of the channels. In an attempt to record from subsynaptic receptors, we have used fast agonist application to study GluR channels in patches excised from dendritic membrane (Stuart, Dodt & Sakmann, 1993). Here we examine the properties of both AMPA and NMDA receptor channels in patches isolated from the apical dendrites of CA3 and CA1 pyramidal neurons, the target of extensive excitatory synaptic input, and compare them with the properties of GluR channels at the soma.

Some of the results have been reported in abstract form (Spruston, Jonas & Sakmann, 1993).

METHODS

Visualization of dendrites and formation of dendritic patches in hippocampal slices

Brains were removed from 13- to 15-day-old Wistar rats killed by decapitation, and transverse hippocampal slices (200–300 μm) were cut in ice-cold physiological saline using a vibrating slicer (FTB, Weinheim, Germany). Where noted in the text, some experiments were also done using 21- to 28-day-old rats. Slices were then incubated at 32–35 °C for 30–60 min and subsequently at room temperature. All experiments were done using an upright microscope (Axioskop FS; Zeiss, Göttingen, Germany) with a ×40 water immersion objective lens (numerical aperture 0·75, working distance 1·9 mm). Outside-out patches from the dendrites and somata of CA3 and CA1 pyramidal neurons were isolated under visual control using infrared differential interference contrast (IR-DIC) videomicroscopy (Stuart *et al.* 1993), utilizing an infrared filter (RG-9; Schott, Germany) and a Newvicon camera (C2400; Hamamatsu, Hamamatsu City, Japan).

Patch pipettes were pulled from borosilicate glass tubing (Hilgenberg, Malsfeld, Germany; 2·0 mm o.d., 0·5 mm wall thickness) and had resistances of 6–15 MΩ when filled with internal solution. Dendrites were approached while positive pressure was applied to the inside of the patch pipette. The pressure was released when a dimple was observed on the dendritic membrane and gentle suction combined with hyperpolarization of the patch pipette resulted in the formation of high-resistance seals (> 10 GΩ) in most cases. After breaking the patch membrane to obtain a whole-cell recording (using a device delivering precisely timed pulses of suction to the inside of the pipette), the series resistance (R_s) was measured from the amplitude of the unfiltered capacitive transient; R_s varied between 20 and 75 MΩ.

Examples of CA3 and CA1 neuron dendrites observed using IR-DIC videomicroscopy are shown in Fig. 1. That the seals were formed on dendritic membrane was confirmed by the fact that the neuron was filled with a fluorescent dye (Lucifer Yellow) contained in the pipette following rupture of the patch (Fig. 1). Although dendritic recordings were not routinely confirmed using fluorescence, a number of other observations suggested that all recordings were made from dendrites; upon breaking the patch membrane, increases in capacitance were observed which were much larger than those expected for small structures such as presynaptic terminals or glial cells that might lie over the dendrite. Resting potentials between −85 and −65 mV were measured in all cases and breakthrough action potentials (large unclamped inward currents) were observed if the cell was depolarized beyond about −50 mV.

Following seal formation and patch rupture, the pipette was withdrawn to form an outside-out patch. The first responses to fast application of glutamate were usually made about 3 min after formation of the whole-cell configuration. Patches often lasted longer than 30 min and occasionally longer than 60 min. No changes in the kinetics of either the AMPA or the NMDA responses were observed during this time, even when run-down of the peak current had occurred.

Fast application

The fast application of agonists was performed as described previously (Colquhoun *et al.* 1992). Double-barrelled application pipettes were fabricated from theta glass tubing (Hilgenberg; 2 mm o.d., 0·3 mm wall thickness, 0·1167 mm septum). Solutions were perfused through control and agonist barrels at a rate of about 0·35 ml min^{-1} by means of a perfusion pump (Infors, Basel, Switzerland), which was modified to hold up to eight 30 ml syringes. The interface between the two solutions was moved across the membrane patch by means of a piezoelectric element (P-245.70; Physik Instrumente, Waldbronn, Germany), upon which the application pipette was mounted. After each patch recording the application was tested by breaking the patch and measuring the open tip current caused by a jump from normal rat Ringer (NRR) solution to 10% NRR. The 20–80% exchange times varied between 50 and 200 μs. Glutamate pulses of 1–7000 ms duration were applied every 2–10 s when isolated AMPA receptor-mediated currents were evoked and every 15–20 s when NMDA currents were investigated. All experiments were performed at room temperature (20–24 °C).

During a recording from one patch, solutions were exchanged using two rotary switching devices having six inflow and six outflow tubes each. One of the outflow tubes from each device was connected to the application pipette. By rotating the input plate, any of the six solutions could be directed to the application pipette. Antagonists were included in both the control and test solutions.

Solutions and drugs

Physiological extracellular solution used for bath perfusion contained (mM): 125 NaCl, 25 NaHCO$_3$, 25 glucose, 2·5 KCl, 1·25 NaH$_2$PO$_4$, 2 CaCl$_2$, 1 MgCl$_2$, and was bubbled with a 95% O$_2$, 5% CO$_2$ gas mixture. The NRR solution used for perfusion of the application pipette contained (mM): 135 NaCl, 5·4 KCl, 1·8 CaCl$_2$, 1 MgCl$_2$, 5 Hepes, with the pH adjusted to 7·2 with NaOH. In most experiments when NMDA receptor-mediated currents were studied, 10 μM glycine was added and Mg^{2+} omitted in the solutions in both barrels of the application pipette. Such solutions are referred to in the text as Mg^{2+}-free, although small amounts of contaminating Mg^{2+} could be present. In experiments for measuring Ca^{2+} permeability, 100 mM CaCl$_2$ with 5 mM Hepes was used as the external solution (pH adjusted to 7·2 with ~2·5 mM Ca(OH)$_2$).

For most experiments the internal solution contained (mM): 130 KCl, 10 EGTA, 10 Hepes, 4 ATP (Mg^{2+} salt), 0·3 GTP (Na$^+$ salt), 10 phosphocreatine (PCr, di-Na$^+$ salt), and 50 units ml^{-1} creatine phosphokinase (CPK); pH was adjusted to 7·3 with KOH (~25 mM). In some patches PCr, CPK, and GTP were omitted from the internal solution and KCl increased by 20 mM to maintain osmolarity; run-down of both AMPA and NMDA components appeared to be greater in these patches. In experiments where measurements were made at potentials positive to −50 mV, CsCl and CsOH were substituted for KCl and KOH in the internal solution. In experiments for measuring Ca^{2+} permeability, 100 mM CsCl was used in the internal solution instead of 130 mM KCl, and CsOH (~25 mM) was used to adjust the pH. Internal solutions containing Lucifer Yellow were prepared by dissolving 8 mg of powder (lithium salt; Sigma, USA) in 40 μl of 100 mM LiCl and adding this to 2 ml internal solution.

L-AMPA (Tocris, Essex, UK) was stored as a 10 mM stock solution in NRR at −20 °C. L-Glutamate and kainate (Sigma) were stored as 100 mM stock solutions in distilled water at −20 °C. The pH of all agonist-containing stock solutions was adjusted to 7·2 using either NaOH or Ca(OH)$_2$. CNQX (Tocris) was stored as a 20 mM stock solution in 0·1 M NaOH at 4 °C. D-AP5 (Tocris) was stored as a 10 mM stock solution in distilled water at −20 °C. These drugs were added to external solutions freshly prepared each day. All other chemicals were from Merck (Darmstadt, Germany), Roth (Karlsruhe, Germany) or Sigma.

Data acquisition and analysis

Currents evoked by fast application of glutamate (or the GluR agonists AMPA and kainate) were recorded using a List EPC-7 amplifier (Darmstadt, Germany) and filtered at 1–10 kHz (−3 dB) using an 8-pole low-pass Bessel filter (Frequency Devices, Haverhill, MA, USA). Currents containing a fast AMPA receptor-mediated component were normally filtered at 3 kHz and isolated slow NMDA receptor-mediated currents at 1–1·5 kHz. Exceptions are noted in the figure legends. All records were digitized using at least twice the filter frequency with an analog-to-digital–digital-to-analog converter board connected to a VMEbus computer system (Motorola Delta series 1147, Tempe, AZ, USA).
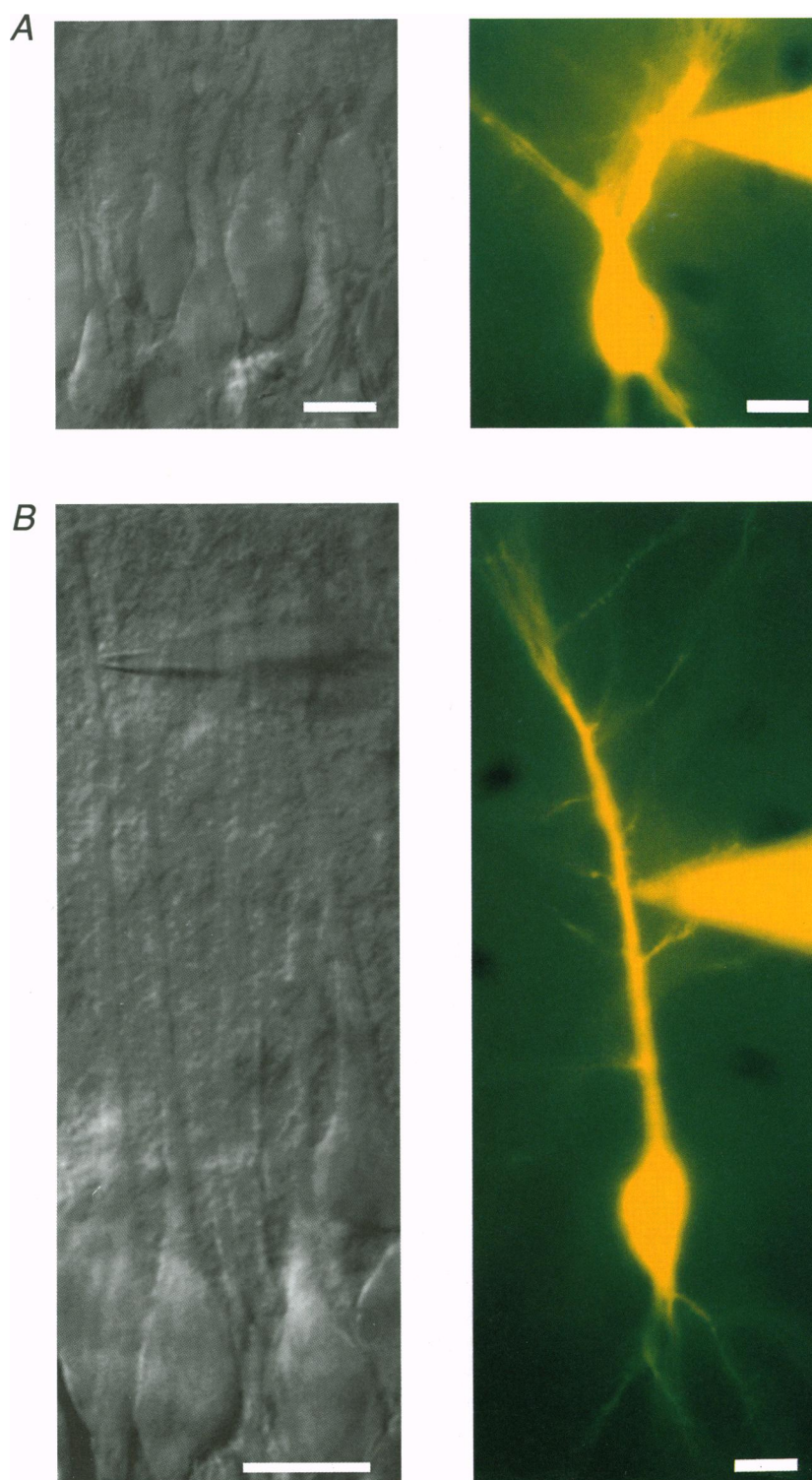
Figure 1. Patch-clamp experiments on apical dendrites of CA3 and CA1 pyramidal neurons in hippocampal slices

A and *B* (left panel), IR-DIC images of the apical dendrites of a CA3 (*A*) and a CA1 (*B*, note patch pipette) pyramidal neuron. *A* and *B* (right panel), photograph of the same CA3 and CA1 cells filled with fluorescent dye (Lucifer Yellow, epifluorescence illumination) via dendritic recording electrodes at distances of 30 and 70 μm from the soma, respectively. Scale bars represent 15 μm.

Analysis and fitting of data was performed using interactive programs running on the VMEbus computer, DISCRETE (S. Provencher, Göttingen, Germany) running on a Sun SPARCstation 2 computer (Sun Microsystems, USA) and Igor (Wavemetrics, Beaverton, OR, USA) and Mathematica (Wolfram Research, Champaign, IL, USA) running on a Macintosh Quadra 800 computer (Apple Computers, USA). The fitting routines in these programs utilize non-linear least squares algorithms. All values are reported as means $\pm$ S.E.M., unless otherwise stated.

Voltage dependence of Mg^{2+} block of NMDA receptor channels

The voltage dependence of the block of NMDA receptor-mediated current in the presence of external Mg^{2+} was described by fitting $I-V$ relationships with the following equation, which assumes a single blocking site for Mg^{2+} within the channel (Woodhull, 1973):

$$I = \frac{I_0}{1 + \frac{[Mg^{2+}]_0}{K_0}\exp(-\delta zFV/RT)}, \qquad (1)$$

where I_0 is the current in Mg^{2+}-free solution, K_0 is the IC_{50} at 0 mV, δ is the electrical distance of the Mg^{2+} binding site from the outside of the membrane, z is the valency of Mg^{2+}, F is the Faraday constant, R is the gas constant, and T is absolute temperature. This method of fitting the $I-V$ relationship for NMDA receptor-mediated currents is not meant to imply a mechanism for the block, but simply provides a practical method for describing the shape of the plot. I_0 was determined from the fit of the $I-V$ relationship in Fig. 4C using the following function, which accounts for the outward rectification observed in nominally Mg^{2+}-free solution:

$$g = g_1 + (g_2 - g_1)/(1 + e^{-\alpha V}), \qquad (2)$$

where g is the conductance, g_1 is the lowest conductance (at very negative potentials) and g_2 is the highest conductance (at very positive potentials), α determines the steepness of the voltage-dependent transition from g_1 to g_2, and $I_0 = g(V - V_{rev})$, where V is the membrane potential and V_{rev} is the reversal potential of the current.

Determination of single-channel conductance

Step transitions corresponding to single AMPA receptor channel gating were sometimes observed but were difficult to measure directly. The properties of single AMPA receptor channels were therefore analysed using non-stationary fluctuation analysis (Sigworth, 1980). Responses to 1 ms pulses of 1 mM glutamate were evoked every 2–3 s in the presence of 30 μM D-AP5. Typically, 50–100 such responses were analysed. To minimize errors due to patch current run-down ($< 25\%$), the variance in each response was determined from the difference of the individual response and a local average of a group of ten responses (Sigworth, 1980). The mean variance (σ^2) determined from all responses was then plotted against the mean current for all responses. The resulting plot can then be fitted with the function (Sigworth, 1980):

$$\sigma^2 = iI - \frac{1}{N}I^2 + \sigma_b^2, \qquad (3)$$

where I is the total current and i is the single-channel current, N is the number of available channels in the patch and σ_b^2 is the variance of the background noise. Single-channel conductance (γ) was then determined as the chord conductance, $\gamma = i/(V_h - V_{rev})$, where V_h is the holding potential and V_{rev} is assumed to be 0 mV. The open probability (P_0) at any time is determined by the equation, $P_0 = I/(iN)$.

Single NMDA receptor currents corresponding to the main conductance state were analysed either by constructing all-points histograms or by setting cursors by eye. These measurements were made from currents evoked by 1 ms pulses of 1 mM glutamate in the presence of CNQX, in the later portions of the responses at times where no more than three superimposed channel openings were observed. Both methods gave identical results.

Determination of Ca^{2+} permeability

The permeability of AMPA- and NMDA-type GluRs to Ca^{2+} was determined from V_{rev} for currents evoked under bi-ionic conditions (external, 102·5 mM Ca^{2+} and internal, 125 mM Cs^+). The relative permeability of Ca^{2+} compared with Cs^+ (P_{Ca}/P_{Cs}) was then calculated from the following equation based on the Goldman–Hodgkin–Katz (GHK) formula (Iino, Ozawa & Tsuzuki, 1990):

$$P_{Ca}/P_{Cs} = \frac{[Cs^+]_i}{4[Ca^{2+}]_0}\exp(FV_{rev}/RT)\,[\exp(FV_{rev}/RT) + 1], \quad (4)$$

where the concentrations are corrected by multiplying by their activity coefficients (0·51 and 0·73 for Ca^{2+} and Cs^+, respectively). No correction for the effects of surface charge screening was made. The measured V_{rev} values reported in the text and Table 1 are not corrected for liquid junction potentials. Before calculating P_{Ca}/P_{Cs}, however, V_{rev} was corrected for two liquid junction potentials that made the measured V_{rev}, 9 mV, too positive (3 mV between the pipette and bath solutions and 6 mV between the 100 mM $CaCl_2$ solution and the bath). Correction for liquid junction potentials decreased P_{Ca}/P_{Cs} values by 30–50%. Correcting for ion activity, on the other hand, had an effect of similar magnitude, but in the opposite direction. The P_{Ca}/P_{Cs} values reported here are therefore roughly comparable to those reported by others who have not corrected for either liquid junction potentials or ion activity.

The fraction of current carried by Ca^{2+} (P_f) under physiological conditions was then estimated from P_{Ca}/P_{Cs} using the following equation (Schneggenburger, Zhou, Konnerth & Neher, 1993, printing error corrected):

$$P_f = \left\{1 + \frac{[M^+]}{[Ca^{2+}]_0}\left[\frac{1 - \exp(2FV/RT)}{4P_{Ca}/P_{Cs}}\right]\right\}^{-1}, \qquad (5)$$

where $[M^+]$ is the total concentration of monovalent cations on each side of the membrane (assumed to be 130 mM and corrected for activity using the coefficient 0·76) and $[Ca^{2+}]_0$ is the concentration of external Ca^{2+} (1·8 mM, corrected for activity using the coefficient 0·58). This equation assumes that the permeability to all monovalent cations is the same and that the relationship between permeability and current can be described by the GHK current equation (see Discussion).

Simulations of EPSCs, EPSPs and Ca^{2+} inflow through GluR channels

Simulations of dual-component EPSCs and excitatory postsynaptic potentials (EPSPs) were performed using NEURON, a program for solving nerve equations (Hines,

1993). The pyramidal neuron modelled consisted of a soma with two equivalent cables corresponding to the apical and basal dendritic trees (see Fig. 16A) which had lengths of 720 and 310 μm, and diameters of 5·0 and 3·8 μm, respectively. Uniform membrane resistivity (R_m, 50 000 Ω cm²), membrane capacity (C_m, 1 μF cm⁻²) and internal resistivity (R_i, 250 Ω cm) were assumed. In addition, fifty spines were explicitly included in the model at each synapse position. Each spine was modelled using two compartments: a spine neck (length 0·8 μm, diameter 0·2 μm) and a spine head (length and diameter, 0·4 μm). Each spine therefore has a surface area of about 1 μm². To account for the additional increase in membrane surface area due to additional spines that were not explicitly modelled, the R_m and C_m values above were halved and doubled, respectively, resulting in an input resistance of 137 MΩ and electrotonic lengths of 0·64 and 0·32 for the apical and basal cables, respectively. Hodgkin–Huxley-like Na⁺ and K⁺ channels were included at a low density in the soma and high density in an axon (length 200 μm, diameter 0·5 μm) attached to the soma.

The AMPA component was modelled as a conductance with a rising time constant of 0·5 ms and a single decay time constant of 3 ms. The NMDA component was modelled with a single exponential rising phase with a time constant of 7 ms and a double exponential decaying phase with time constants of 200 and 2000 ms, contributing 80 and 20 % to the total decay amplitude, respectively. The voltage dependence of the NMDA receptor channels was modelled using eqns (1) and (2).

The fraction of the current through NMDA receptor channels that was carried by Ca²⁺ was determined by multiplying the current by P_f (see eqn (5)). In order to avoid numerical instabilities where P_f approaches infinity, the reversal potential of the modelled NMDA current was set equal to that predicted by the assumptions used for eqn (5) (V_{rev}, +1·5 mV).

RESULTS

Dual-component responses to brief glutamate pulses

In CA3 pyramidal cells, the site of recording was between the first and third branch points at distances between 15 and 76 μm from the border of the pyramidal cell body layer (mean distance, 40 μm, $n = 92$). The recording site was therefore located in the stratum lucidum in a region where mossy fibre (MF) boutons form synapses on CA3 pyramidal neuron dendrites (Johnston & Brown, 1983). In CA1 pyramidal cells, seals could be formed at greater distances from the soma and recordings were obtained between 25 and 174 μm from the border of the pyramidal cell layer (mean distance, 64 μm, $n = 72$). This corresponds to a region in the stratum radiatum where SC synapses are formed.

Responses of dendritic membrane patches were first studied using brief glutamate pulses to mimic the synaptic release of glutamate (Clements, Lester, Tong, Jahr & Westbrook, 1992). Experiments were carried out in Mg²⁺-free external solution containing 10 μM glycine to provide optimal conditions for the activation of NMDA-type GluR channels.

Time course. Currents activated by 1 ms pulses of 1 mM glutamate in both CA3 and CA1 dendritic patches had two clearly distinguishable components; an initial, rapidly rising and decaying component and a second, more slowly decaying component (Fig. 2A). The rapid rise and decay of the early initial component suggested that it was mediated by AMPA- and/or kainate-type GluR channels, while the slower time course and large single-channel openings in the decay of the second component suggested that it was mediated by NMDA-type GluR channels.

Effects of specific antagonists. The identity of the two components was confirmed using the AMPA/kainate receptor antagonist CNQX and the NMDA receptor antagonist D-AP5. As shown in Fig. 2A and B, the early component could be blocked completely by 5 μM CNQX. In the same patch, the late, slow component could be abolished by 30 μM D-AP5 (Fig. 2A and C). Results were similar for both CA3 and CA1 dendritic patches. Block by both CNQX and D-AP5 developed rapidly and was fully reversible (data not shown). The different time course of the two pharmacologically isolated components is illustrated on a faster time scale in Fig. 2D.

Relative amplitudes. As shown by the examples in Fig. 3A and B, the size of the slow component (mean value in a 10–15 ms window beginning 10–25 ms after the peak of the fast component) relative to that of the fast component varied considerably between different patches (0·03–0·62 in CA3 dendritic patches and 0·03–0·54 in CA1 dendritic patches). A scatter plot of the maximum amplitude of the slow component against the amplitude of the fast component is shown for CA3 and CA1 patches in Fig. 3C and D, respectively. The average relative amplitude of the slow component compared to that of the fast component was 0·22 ± 0·03 ($n = 26$) for CA3 and 0·21 ± 0·03 ($n = 20$) for CA1 dendritic patches.

Voltage dependence. Figure 4 shows I–V relationships of the fast and slow components of the glutamate-activated currents. In Mg²⁺-free solution containing 10 μM glycine, the I–V curves of both components displayed slight outward rectification and had reversal potentials near 0 mV (Fig. 4B, fast component; C, slow component). In external solution containing 1 mM Mg²⁺ and 10 μM glycine, the amplitude of the fast component remained slightly outwardly rectifying, whereas the amplitude of the slow component was smaller at negative potentials than at more positive potentials (Fig. 4D). Accordingly, the I–V of this component had a region of negative slope conductance between −80 and −20 mV (Fig. 4F). The maximum inward current of the slow component occurred at −20 mV ($n = 3$ CA3 dendritic patches). The strong voltage dependence of the slow component in the presence of external Mg²⁺ provides further evidence that this current is mediated by NMDA-type GluR channels (Nowak, Bregestovski, Ascher, Herbert & Prochiantz, 1984). The properties of the fast component are consistent with it being mediated by AMPA- and/or kainate-type GluR channels.

Comparison of responses to glutamate, AMPA and kainate

The agonist preference of the GluR channels underlying the fast, CNQX-sensitive component was examined in the absence of glycine and in the presence of Mg^{2+} in the external solution by comparing the currents activated by 100 ms glutamate pulses with those activated by AMPA and kainate. As shown in Fig. 5, the response to a 100 ms pulse of 1 mM AMPA was similar, but not identical, to that evoked by a 100 ms pulse of 1 mM glutamate. Identical results were observed in two CA3 and two CA1 dendritic patches in which these three agonists were compared. The currents evoked by either AMPA or glutamate desensitized substantially during the 100 ms agonist pulse. In contrast to the AMPA and glutamate responses, 100 ms pulses of 1 mM kainate evoked small, weakly desensitizing currents, even when applied at very low rates (0·017–0·1 Hz) to allow enough time for recovery from desensitization. The absence of a pronounced desensitizing component of the kainate response was observed in a total of ten patches from both CA3 and CA1 dendrites and somata. The recovery from desensitization of AMPA- or glutamate-activated currents also differed from that of kainate-activated currents. Responses to AMPA and glutamate recovered from desensitization rather slowly, as indicated by the reduced response to a second pulse of agonist 50 ms following the end of the first pulse (Fig. 5). The second application of kainate, however, produced a response that was almost identical to the first (Fig. 5). The most likely interpretation of these results is that the current evoked by glutamate is due to its action on AMPA-preferring receptors, probably assembled from subunits of the GluR-A to D family (see Discussion).

Conductance and permeability of AMPA receptor channels

The properties of the AMPA receptor-mediated component were studied in isolation in the absence of glycine and in the presence of 1 mM Mg^{2+} and 30 μM D-AP5 in the external solution.

Conductance. The single-channel conductance of AMPA receptor channels (γ) was estimated using non-stationary fluctuation analysis of responses to 1 ms pulses of 1 mM glutamate (Sigworth, 1980). The results of such an analysis

Figure 2. Pharmacological separation of the fast and slow components in the response to 1 ms pulses of 1 mM glutamate

A, currents activated in the absence of Mg^{2+} and presence of 10 μM glycine (average of 10 sweeps). The duration of the glutamate application is indicated here and in subsequent figures by the open tip response recorded at the end of the experiment (upper traces; see Methods). *B*, addition of 5 μM CNQX blocked the fast component without affecting the slow component (average of 36 sweeps). *C*, addition of 30 μM D-AP5 blocked the slow component without affecting the fast component (average of 10 sweeps). Note the faster time base than in *A* and *B*.

D, pharmacologically isolated fast and slow components superimposed on the same time base. All data are from a CA1 dendritic patch formed at a distance of 44 μm from the soma (V_h was −80 mV).
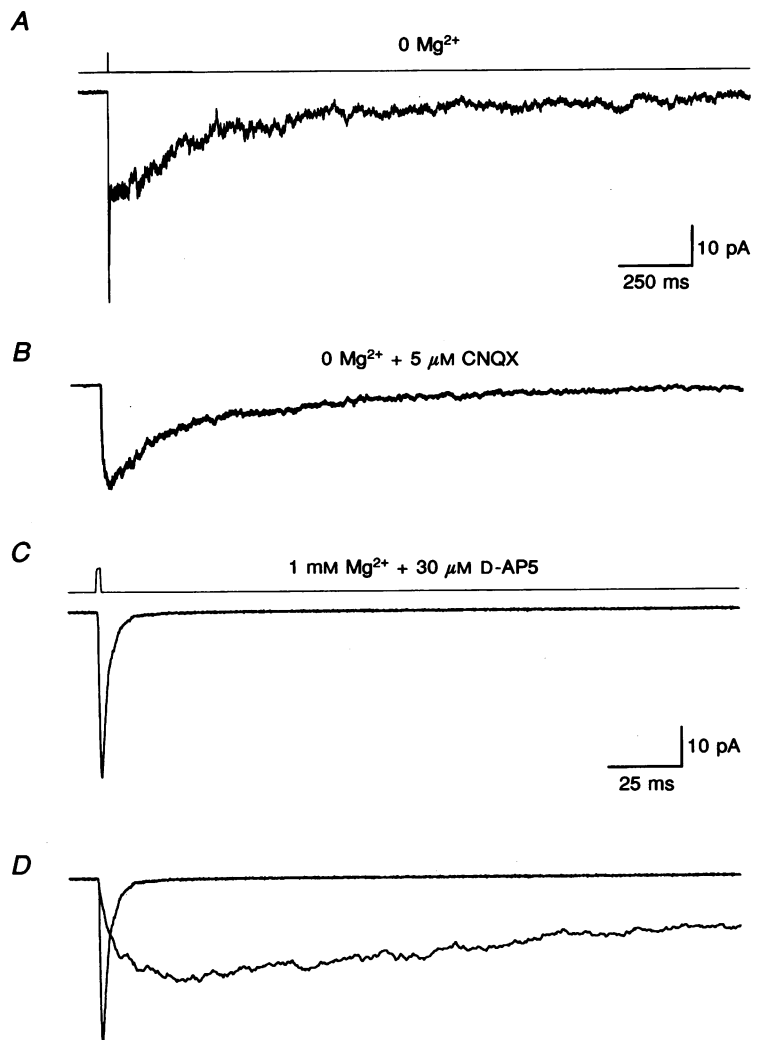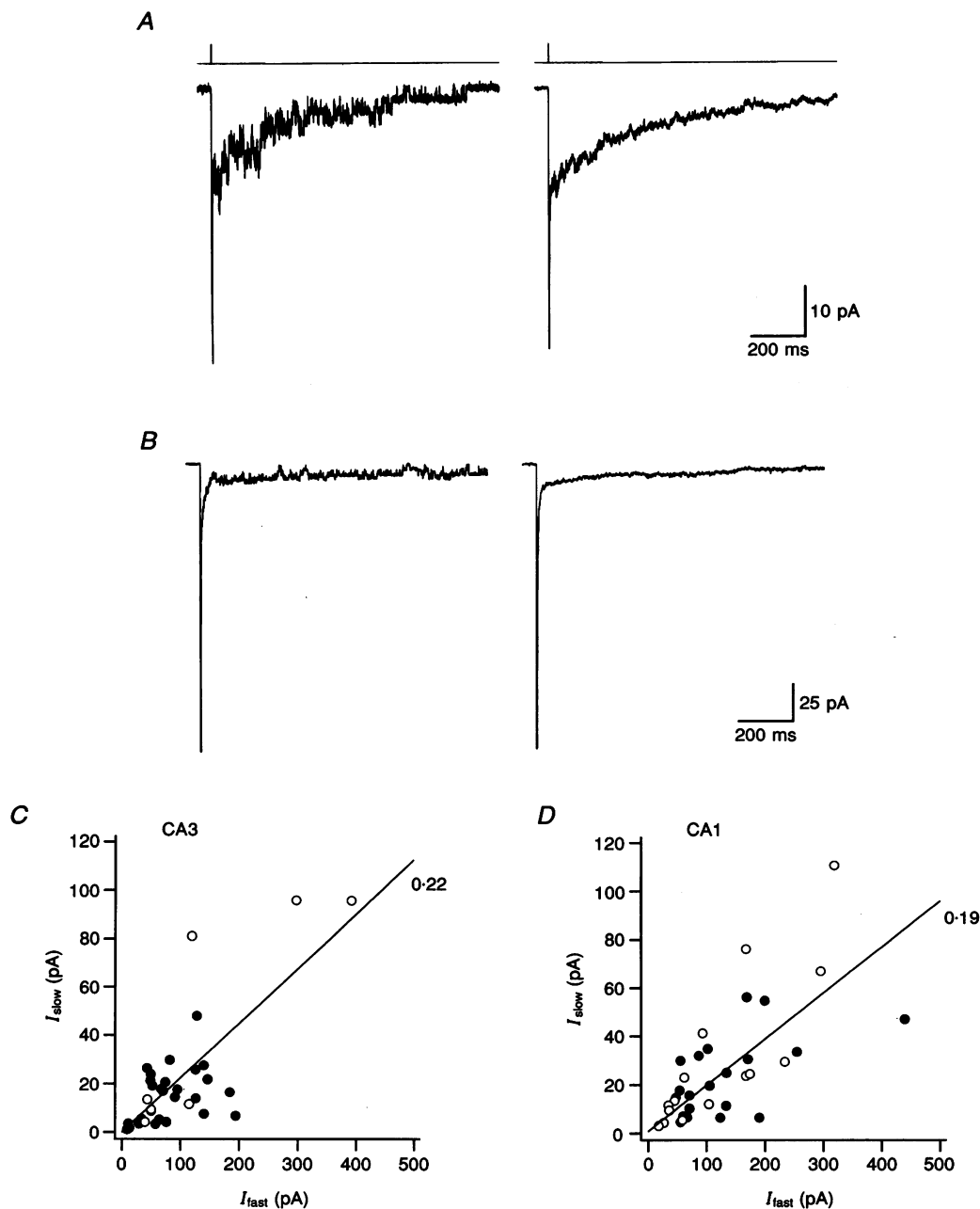
Figure 3. Relative size of NMDA and AMPA receptor-mediated currents in dual-component glutamate responses varies between patches

A, example of a CA3 dendritic patch with a relatively large slow component. *B*, example of another CA3 dendritic patch with a relatively small slow component. Individual sweeps (left panel) and averages of 9–10 sweeps (right panel) are shown in *A* and *B*. Traces shown are from CA3 dendritic patches taken at distances of 30 (*A*) and 45 μm (*B*) from the border of the stratum lucidum. *C* and *D*, scatter plots of amplitude of the slow (I_{slow}) component against amplitude of the fast (I_{fast}) component of the current activated by 1 ms pulses of 1 mM glutamate in different membrane patches from CA3 (*C*) and CA1 (*D*) dendrites (●) and somata (○). The indicated slopes beside the regression lines through all points (and the origin) represent the mean ratio of I_{slow} to I_{fast} for all dendritic and somatic patches. In all cases, solutions contained 10 μM glycine and no added Mg^{2+} (V_h was −80 mV).
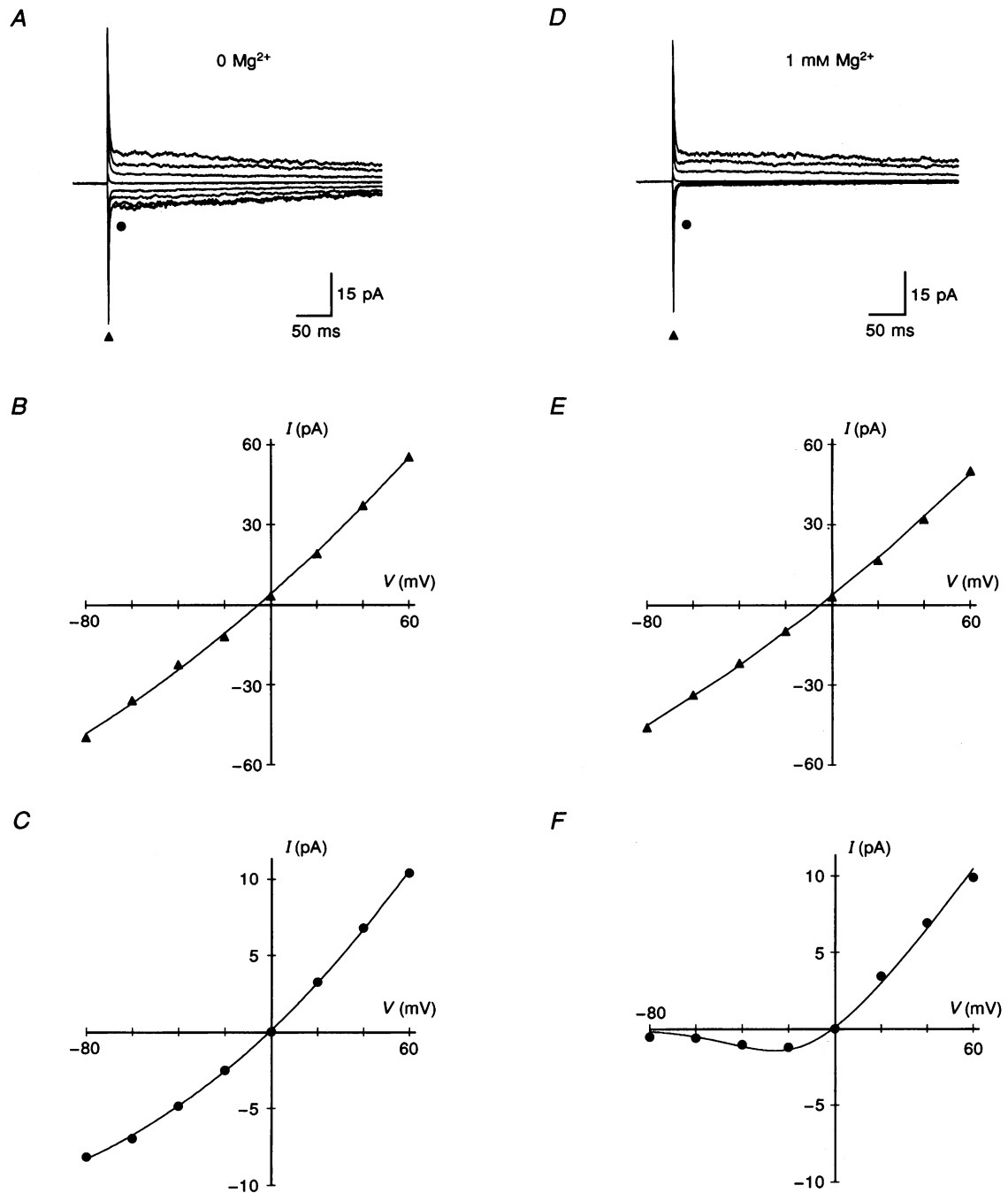
Figure 4. Current–voltage relationships of the fast and slow phases of the dual-component response from a CA3 dendritic patch

A, currents evoked by 1 ms pulses of 1 mM glutamate in solution containing 10 μM glycine and no added Mg^{2+}. B and C, I–V relationships for the fast (B; peak, ▲) and slow (C; mean current 15–25 ms after the peak, ●) currents shown in A. D, currents were obtained in external solution containing 1 mM Mg^{2+}. E and F, I–V relationships for fast and slow currents shown in D. Each trace is the average of 17–24 sweeps (V_h was −80 to +60 mV, 20 mV steps). All data are from a CA3 dendritic patch taken at a distance of 76 μm from the border of the stratum lucidum. I–V relationships in B and E were fitted using second-order polynomials yielding V_{rev} values of −5·2 and −4·7 mV, respectively. The I–V relationship in C was fitted with eqn (2) ($g_1 = 40$ pS, $g_2 = 247$ pS, $\alpha = 0·01$, $V_{rev} = -0·7$ mV). The I–V relationship in F was fitted with eqn (1) ($K_0 = 4·1$ mM, $\delta = 0·8$, $V_{rev} = -0·7$ mV). The half-maximal inhibitory concentration (IC_{50}) of Mg^{2+} calculated from this fit was 24 μM at a V_h of −80 mV.

Table 1. Comparison of the properties of AMPA and NMDA receptor-mediated currents in hippocampal membrane patches

	CA3 dendrites	n	CA3 somata	n	CA1 dendrites	n	CA1 somata	n
AMPA-type GluR								
γ (pS)	9.8 ± 0.7	3	—		10.2 ± 0.8	7	—	
N	321 ± 158	3	—		291 ± 55	7	—	
$P_{0,\,max}$	0.48 ± 0.04	3	—		0.57 ± 0.06	7	—	
Ca^{2+}/Cs^{+} reversal (mV)	-49.9 ± 0.8	4	—		-48.1 ± 0.7	3	—	
Deactivation τ_1 (ms)	1.8 ± 0.2 (83%)	23	1.7 ± 0.2 (79%)	10	2.2 ± 0.2 (83%)	18	2.2 ± 0.2 (78%)	10
Deactivation τ_2 (ms)	8.1 ± 1.5 (17%)	23	6.3 ± 1.0 (21%)	10	9.0 ± 1.2 (17%)	18	6.8 ± 0.6 (22%)	10
Desensitization τ_1 (ms)	9.2 ± 1.0 (55%)	16	10.1 ± 1.7 (55%)	6	9.6 ± 0.4 (66%)	13	8.5 ± 0.7 (60%)	18
Desensitization τ_2 (ms)	33.5 ± 3.8 (45%)	16	39.7 ± 8.5 (45%)	6	34.8 ± 2.2 (34%)	13	33.6 ± 2.8 (40%)	18
NMDA-type GluR								
γ (pS)	46.3 ± 0.6	3	—		43.5 ± 0.7	3	—	
Ca^{2+}/Cs^{+} reversal (mV)	31.4 ± 0.7	6	—		31.6 ± 0.8	5	—	
Activation τ (ms)	6.0 ± 0.5	13	4.8 ± 0.5	10	8.8 ± 0.6	23	7.8 ± 0.8	10
Deactivation τ_1 (ms)	175 ± 20 (72%)	13	197 ± 24 (82%)	10	288 ± 23 (78%)	23	230 ± 36 (85%)	10
Deactivation τ_2 (ms)	1188 ± 181 (28%)	13	1287 ± 129 (18%)	10	2824 ± 253 (22%)	23	2918 ± 491 (15%)	10
Desensitization τ (ms)	601 ± 112	5	—		457 ± 60	12	—	

All data are from responses to 1 mM glutamate as described in the text. Values given are means $\pm$ S.E.M. All time constants (τ) were determined at -80 mV. Percentages of fit amplitude corresponding to each τ are given in parentheses. Isolated AMPA components were studied in 1 mM Mg^{2+}, 0 glycine and 30 μM D-APV. Isolated NMDA components were studied in 0 Mg^{2+}, 10 μM glycine and 5 μM CNQX. Reversal potentials are not corrected for junction potentials (see Methods). *N*, number of channels; *n*, number of patches tested.

are shown in Fig. 6. Ten responses and their mean are shown in *A*. In *B*, the difference between each of these sweeps and the mean is shown. From these differences, the average variance as a function of time is plotted in *C*. Finally, a plot of the variance *versus* the mean current for a total of ninety sweeps is shown in *D*. This plot was generated by averaging the plots of variance *versus* time (*C*) for nine groups of ten responses and plotting this average variance against the grand average of the mean currents. The plot in Fig. 6*D* is fitted with a parabola (see Methods, eqn (3)) to yield estimates of γ and the number of channels in the patch (*N*). Data from CA3 ($n = 3$) and CA1 dendritic patches ($n = 7$) resulted in similar values for γ of about 10 pS, with an average of about 300 available channels in the patch (Table 1). The probability of any

given channel being open at the peak of the response ($P_{0,\,max}$) was, on average, between 0.5 and 0.6 (see Table 1). The γ value is similar to that estimated for AMPA receptor channels in the soma of CA3 neurons (Jonas *et al.* 1993) and neocortical pyramidal neurons (Hestrin, 1993), but lower than in neocortical interneurons (Hestrin, 1993) or for synaptic currents in cerebellar granule neurons (Traynelis, Silver & Cull-Candy, 1993).

In order to test the ability of the non-stationary fluctuation analysis to determine the correct γ and *N* values, a kinetic model of the AMPA receptor channel (Jonas *et al.* 1993) was used to simulate responses to 1 ms pulses of 1 mM glutamate. Experimental conditions were reproduced by generating fifty to a hundred responses, with run-down simulated by reducing the number of available channels by one on each subsequent

Figure 5. Comparison of the responses to glutamate, AMPA and kainate

Superimposed responses to two 100 ms agonist pulses separated by a 50 ms interval are shown for 1 mM glutamate, 1 mM AMPA and 1 mM kainate. Currents were recorded in the presence of 1 mM Mg^{2+} and 30 μM D-AP5, and in the absence of glycine. Each trace is an average of 10 sweeps (V_h was -80 mV). Data are from a CA1 dendritic patch taken at a distance of 74 μm from the soma.
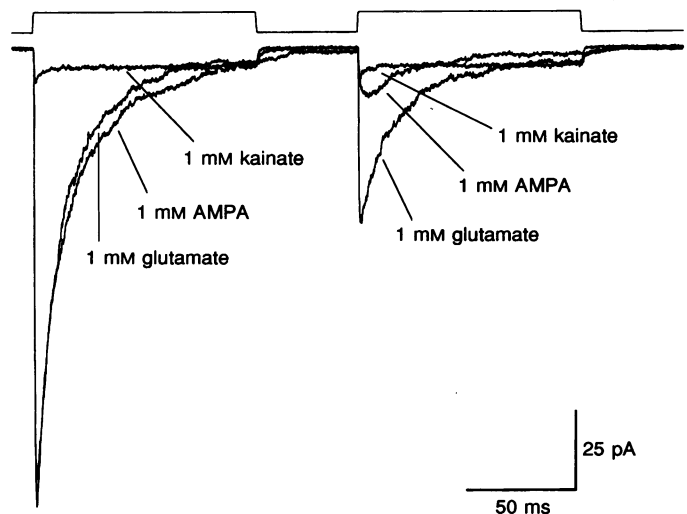
sweep, so that a total of 20% run-down occurred. These data were then analysed in the same way as experimental data. The simulations suggest that the experimental data described above should provide mean γ and N estimates in error by no more than 10%. These estimates represent a weighted mean of all main and subconductance states of the channels in the patch (Cull-Candy, Howe & Ogden, 1988).

Ca^{2+} permeability. The permeability of the AMPA receptor channels to Ca^{2+} was studied with an external solution containing 102·5 mM Ca^{2+} and an internal solution containing 125 mM Cs^+. An example of such an experiment is shown in Fig. 7. Under these conditions, the measured V_{rev} for currents evoked by 1 ms pulses of 1 mM glutamate was about −50 mV (Table 1), compared with −4·6 mV in normal external solution (arrow, Fig. 7B). The relative permeabilities of the channels to Ca^{2+} and Cs^+ (P_{Ca}/P_{Cs}; see

Methods) were 0·047 and 0·051 for CA3 and CA1 dendritic patches, respectively. These results suggest that the AMPA-type GluRs in hippocampal pyramidal cell dendrites have a relatively low, but measurable, permeability to Ca^{2+} (see Discussion).

Conductance and permeability of NMDA receptor channels

The functional properties of the NMDA receptor-mediated component were studied in isolation in Mg^{2+}-free solution containing 5 μM CNQX and 10 μM glycine. This appeared to be a saturating concentration of glycine because the peak NMDA response in 1 μM glycine was 95 ± 2% of that in 10 μM glycine ($n = 3$ CA1 dendritic patches). Responses were extremely small or undetectable in the absence of added glycine.
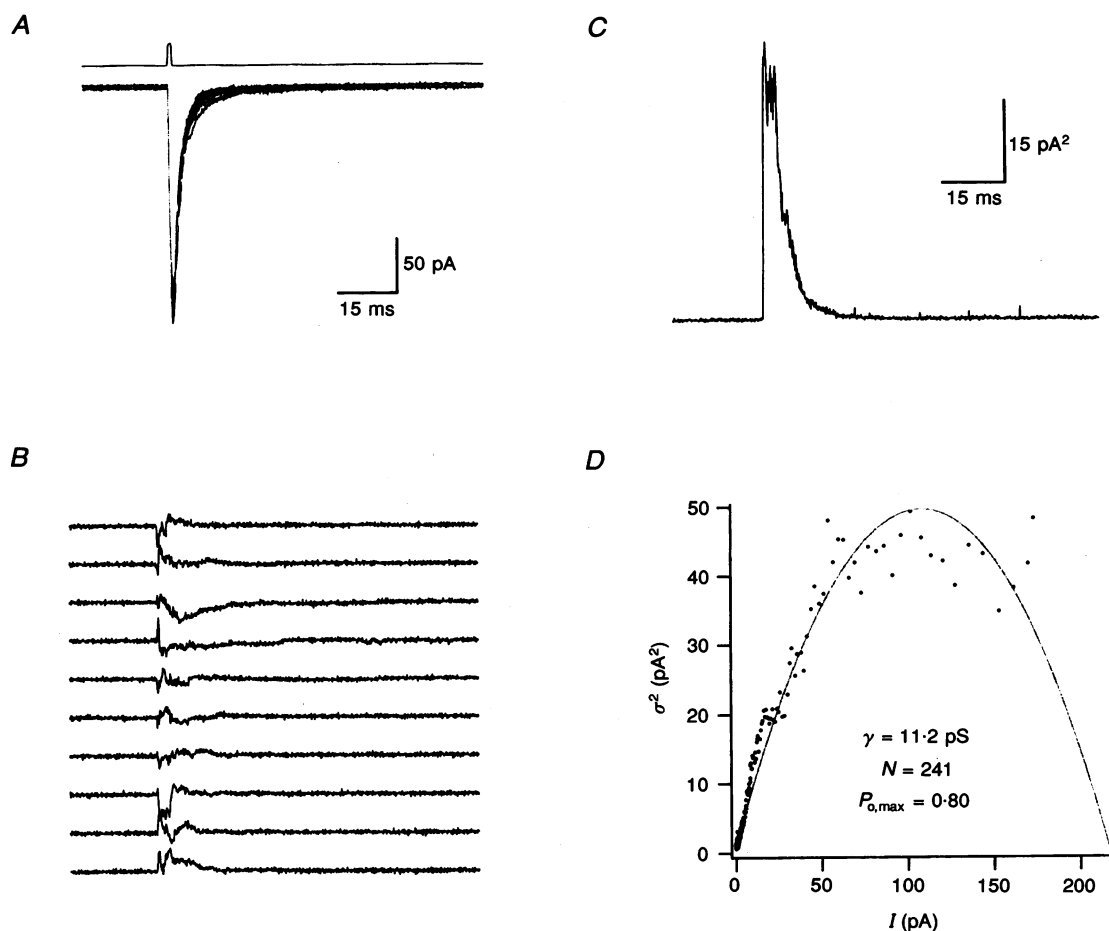
Figure 6. Properties of single AMPA receptor channels determined using non-stationary fluctuation analysis

A, 10 individual current responses to 1 ms pulses of 1 mM glutamate are superimposed on the local mean (of the same 10 responses, grey line). Responses were obtained in solution containing 30 μM D-AP5 and 1 mM Mg^{2+} (V_h was −80 mV). B, difference of each individual response in A from the local mean. C, mean variance (with respect to the local mean) plotted *versus* time for the 10 responses in A. D, plot of the mean variance for a total of 90 responses obtained in this patch as a function of the mean current for all 90 responses. The data are fitted with eqn (3) (see Methods) to determine γ, N and $P_{o,max}$. In this experiment the data were filtered at 5 kHz and sampled at 10 kHz. Data were from a CA1 dendritic patch taken at a distance of 42 μm from the soma.

Conductance. Examples of single NMDA receptor channel currents activated by 1 ms pulses of 1 mM glutamate are shown in Fig. 8A and the corresponding all-points histogram of several traces is shown in Fig. 8B. Single-channel I–V relationships for the main conductance state were approximately linear in the absence of Mg^{2+} (Fig. 8C). Fits of single-channel I–V curves with a linear function revealed a mean elementary conductance of about 45 pS for both CA3 and CA1 dendritic patches (Table 1). This value is similar to that reported for acutely dissociated hippocampal neurons at physiological external Ca^{2+} concentrations (Gibb & Colquhoun, 1992). Subconductance states were often observed but were not analysed in detail.

Ca^{2+} permeability. The permeability of the NMDA receptor channels to Ca^{2+} ions was studied with an external solution containing 102·5 mM Ca^{2+} (Mg^{2+}-free, with 10 μM glycine) and an internal solution containing 125 mM Cs^+. An example of this type of experiment is shown in Fig. 9. Under these conditions the mean V_{rev} of currents evoked by 1 ms pulses of 1 mM glutamate was about +30 mV (Table 1), compared with −0·8 mV in normal external solution (arrow, Fig. 9B). Similar values have been reported by others (Ascher & Nowak, 1988; Jahr & Stevens, 1993). After correcting for activity of the ions in solution as well as liquid junction potentials (see Methods), the P_{Ca}/P_{Cs} ratios calculated from these V_{rev} values were 3·6 for both CA3 and CA1 dendritic patches, respectively, which is about 100-fold higher than the Ca^{2+} permeability of AMPA-type GluRs. The single-channel chord conductance

at negative potentials in 102·5 mM Ca^{2+} external solution was about one-third that in normal external solution (data not shown), suggesting that Ca^{2+} is a less effective charge carrier through NMDA receptor channels than are monovalent cations (see also Ascher & Nowak, 1988; Jahr & Stevens, 1993).

Time course of AMPA receptor-mediated currents

Brief glutamate pulses evoked AMPA receptor-mediated currents that rose rapidly to a peak and decayed within about 10 ms. Longer glutamate pulses produced identical peak currents that almost completely desensitized during the continued application of agonist. Figure 10 illustrates the differences in time course of currents elicited by 1, 10 and 100 ms pulses of 1 mM glutamate.

Rise time course. As shown in Fig. 10B, the complete time course of the current evoked by a 1 ms pulse of 1 mM glutamate could be approximately described by the sum of one rising and one decaying exponential. The rising phase in this case had a time constant of 0·55 ms (20–80% rise time 223 μs). In all patches and for all pulse lengths the 20–80% rise time was in the range of 200–600 μs.

Deactivation time course. The deactivation of the current response to 1 ms pulses of 1 mM glutamate (Fig. 10B; also referred to as *offset*, e.g. Colquhoun *et al.* 1992) was much faster than that of the desensitization observed during 100 ms pulses (Fig. 10C). After a 1 ms pulse, the current decayed with a time constant of about 3 ms (τ was 2·7 ± 0·2 ms for 25 CA3 dendritic patches;
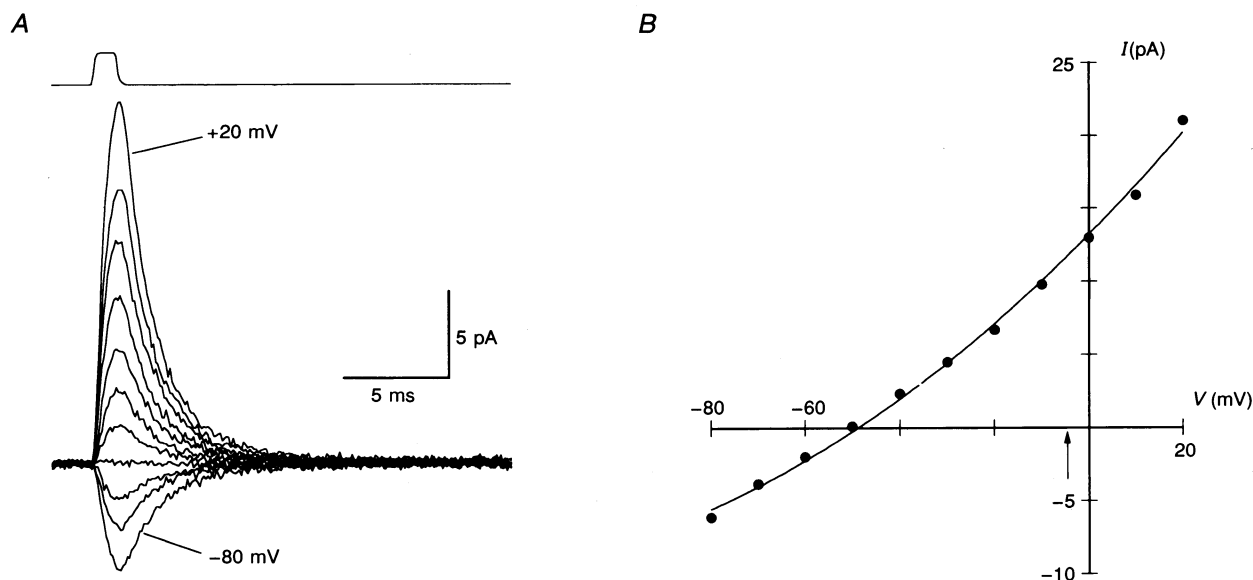
Figure 7. Ca^{2+} permeability of AMPA receptor channels

A, currents evoked by 1 ms pulses of 1 mM glutamate in external solution containing 102·5 mM Ca^{2+} and 30 μM D-AP5 (125 mM Cs^+ in the pipette). Each trace is the average of 7–12 sweeps (V_h was −80 to +20 mV, 10 mV steps). B, I–V relationship of the peak currents shown in A. The reversal potential calculated from the second-order polynomial fit shown is −49 mV. The arrow indicates the mean reversal potential measured from other patches in normal external solution. All data are from a CA1 dendritic patch taken at a distance of 40 μm from the soma.

2·6 ± 0·2 ms for 11 CA3 somatic patches; 3·0 ± 0·2 ms for 20 CA1 dendritic patches; and 2·8 ± 0·2 ms for 20 CA1 somatic patches). As shown previously (Colquhoun *et al.* 1992), there appeared to be little or no voltage dependence of this parameter. In most patches, a two-exponential fit of the decay provided a somewhat better fit of the deactivation time course. This can be seen in Fig. 10*B*, where the single-exponential fit deviates from the data at later times. Fitting the deactivation with two exponentials resulted in a faster dominant component ($\tau_1 \approx 2$ ms, ~80% of the amplitude; $\tau_2 \approx 8$ ms, ~20%; see Table 1). The existence of two components may be a kinetic property of the channels (e.g. one component due to direct transitions from an open to a closed state and one component due to transitions from a desensitized to an open to a closed state) or may be due to the existence of two types of channels
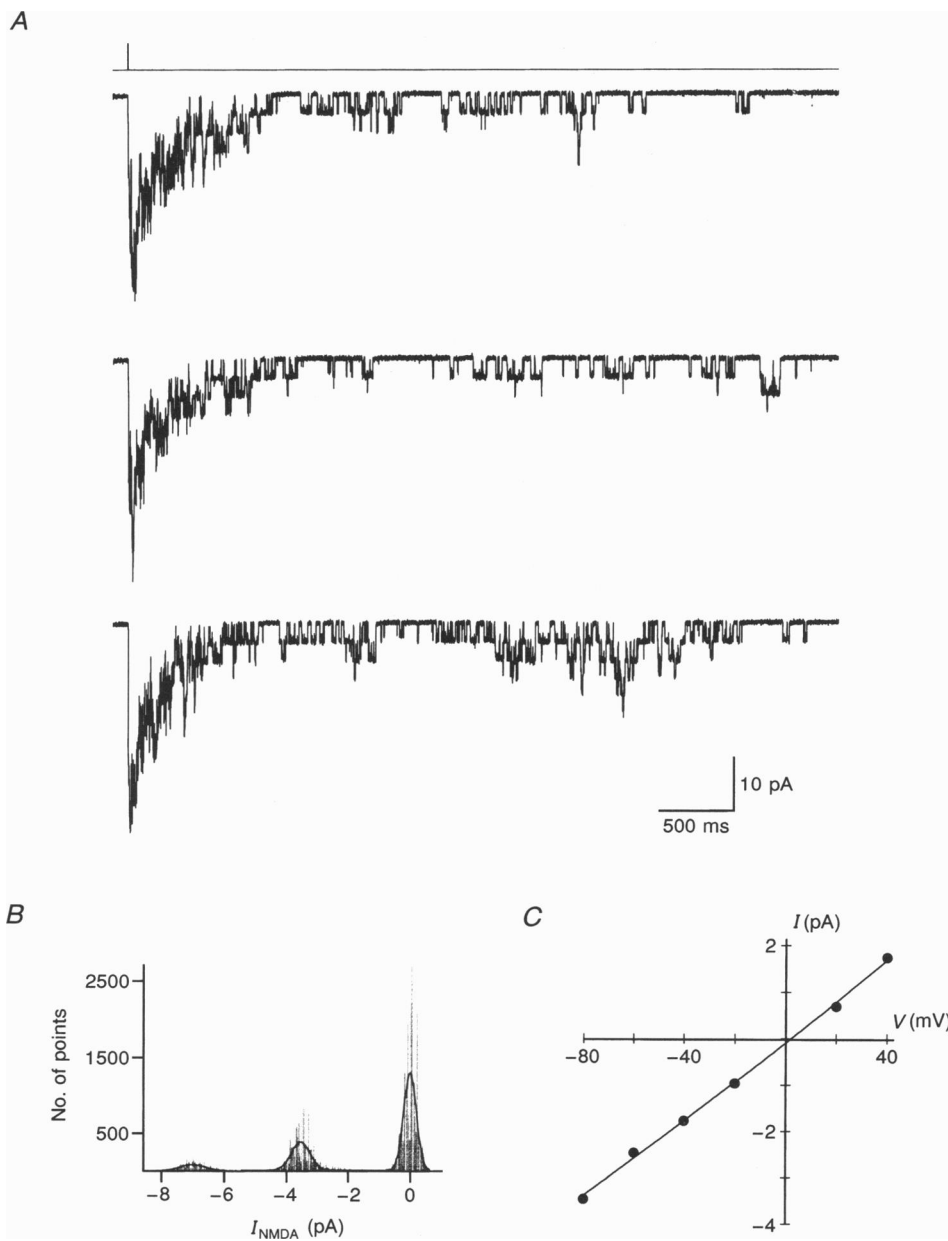
Figure 8. Properties of single NMDA receptor channels

A, individual responses to 1 ms pulses of 1 mM glutamate in solution containing 10 μM glycine, 5 μM CNQX and no added Mg^{2+} (V_h was −80 mV). *B*, histogram of points beginning 500 ms after the glutamate pulse for the 3 sweeps shown in *A*. Each of the 3 peaks was fitted with a Gaussian distribution, yielding mean values of 0, −3·54 and −6·99 pA. *C*, *I*–*V* relationship for single channels in the same patch. Each point represents the mean for measurements made from 5 sweeps (S.E.M. were smaller than the symbols). The single-channel conductance calculated from the slope of a straight line fitted to the points was 43 pS and the reversal potential was +2·1 mV. Data are from a CA1 dendritic patch formed at a distance of 44 μm from the soma.

with different kinetic properties. If two types of channels exist, they are not likely to reflect a difference in the behaviour of synaptic and extrasynaptic channels, since both components of the deactivation were observed in both dendritic and somatic patches.

Desensitization time course. During 100 ms glutamate pulses, in both CA3 and CA1 dendritic patches, the current decayed with a double exponential time course having time constants of about 10 and 34 ms, accounting for about 60 and 40% of the total current amplitude, respectively (Table 1, e.g. Fig. 10*C*). The difference in the time course of deactivation and desensitization can be seen by the two temporally distinct decay phases in the current response to 10 ms glutamate pulses (Fig. 10*A*). No differences in the deactivation and desensitization kinetics of AMPA receptor-mediated current kinetics were observed either

between dendritic and somatic patches or between CA3 and CA1 patches (analysis of variance, ANOVA, $P > 0.05$).

Time course of NMDA receptor-mediated currents

Brief glutamate pulses evoked NMDA receptor-mediated currents that rose to a peak and decayed over a period of seconds. Longer glutamate pulses produced slightly larger peak currents that then partially desensitized during the continued application of agonist. Figure 11 illustrates the differences in time course of currents elicited by 1 ms, 1 s and 7 s pulses of 1 mM glutamate.

Rise time course. The rise time of the NMDA receptor-mediated current evoked by 1 ms glutamate pulses was very slow relative to that of the AMPA component. Because the 20–80% rise time poorly characterized this slow rise, both the rising and decaying phases of the current were fitted with the sum of three exponentials; one describing the

A

B
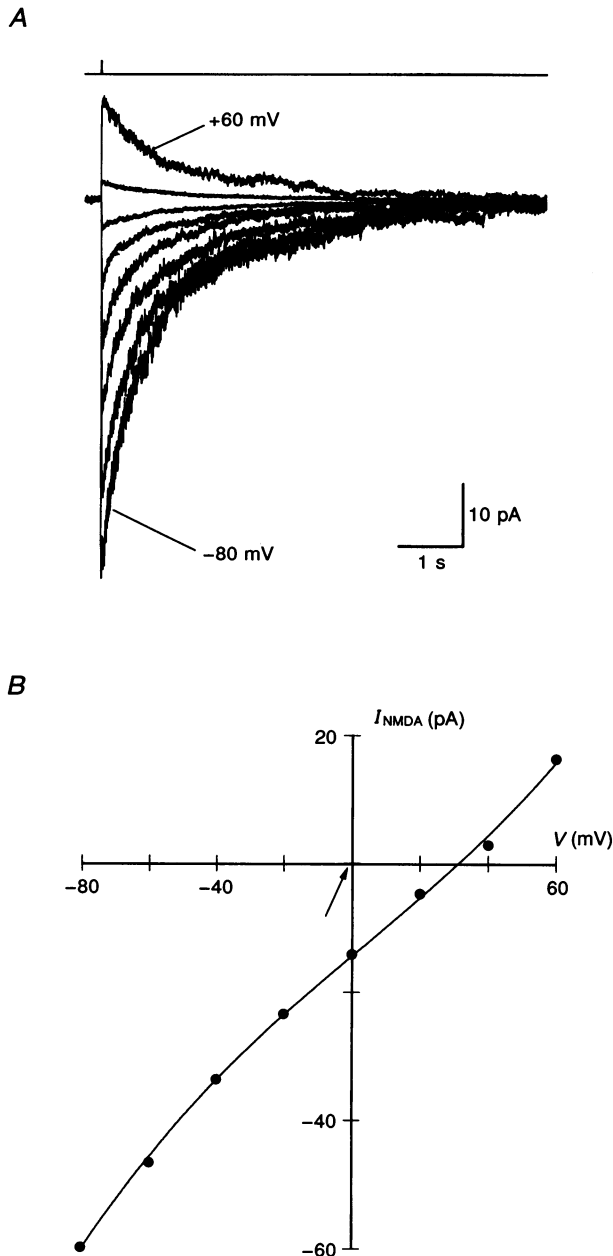
Figure 9. Ca^{2+} permeability of NMDA receptor channels

A, currents evoked by 1 ms pulses of 1 mM glutamate in solution containing 102·5 mM Ca^{2+}, 10 μM glycine, 5 μM CNQX, and no added Mg^{2+} (125 mM Cs^{+} in the pipette). Each trace is the average of 5 sweeps (V_h was −80 to +60 mV, 20 mV steps). *B*, *I–V* plot of the currents shown in *A*. The reversal potential calculated from the second-order polynomial fit shown is +28 mV. The arrow indicates the mean reversal potential measured from other patches in normal external solution. All data are from a CA1 dendritic patch taken at a distance of 65 μm from the soma.

rising phase and two describing the decaying phase (Fig. 11B). The time constant of the rising phase was about 7 ms in both CA3 and CA1 dendritic patches (Table 1). The time to peak determined from the fits of the currents was about 20–30 ms, indicating that the maximum current occurs at a time well after the glutamate concentration and the AMPA receptor-mediated current have decayed to zero.

Deactivation time course. At least two exponentials were required to describe the decay of the average NMDA receptor-mediated currents in response to 1 ms pulses of 1 mM glutamate (Fig. 11B). The fast component of the decay had a time constant of about 150–250 ms and the slow component about 1 s in CA3 and about 3 s in CA1 dendritic patches (Table 1). The slow component of the NMDA receptor-mediated current accounted for about 20% of the total current amplitude in both CA3 and CA1 dendritic and somatic patches (Table 1). Both the fast and the slow components of the NMDA receptor-mediated current decay were slower in CA1 neurons than in CA3 neurons, but only the difference in the slow component was statistically significant (ANOVA, with Tukey's multiple comparisons, $P < 0.05$).

A number of tests were performed to exclude the possibility that the slow decay of the NMDA receptor-mediated currents was an artifact of the solution exchange. Firstly, the open tip response (with 10% NRR in the agonist barrel) was examined at high gain; the current 10 ms after the end of the pulse was only 0·025% of the maximum, implying that 1 mM glutamate would have decayed to below 250 nM by this time. Secondly, if the patch pipette was moved from close to the interface to the centre of the control barrel (about 50 μm away from the interface) immediately after each application of 1 mM glutamate, the resulting currents had the same time course as those evoked in the usual way. Thirdly, 100 μM glutamate was used instead of 1 mM glutamate as the agonist. This 10-fold decrease in agonist concentration did not eliminate the slow component of the decay of the NMDA receptor-mediated current. Finally, a difference in the time constant of the slow component of the NMDA receptor-mediated current decay was observed between CA3 and CA1 dendritic patches despite identical application conditions. All of these tests indicate that the decay of the NMDA receptor-mediated currents was unlikely to be prolonged by low levels of glutamate persisting at the patch following movement of the application pipette.

Desensitization time course. Longer glutamate pulses produced desensitizing NMDA receptor-mediated currents. This desensitization was not as complete as for the AMPA receptor-mediated component; at the end of 2–7 s pulses, a steady-state current of $0·21 \pm 0·02$ ($n = 5$) and $0·33 \pm 0·03$ ($n = 12$) of the peak response was observed in CA3 and CA1 dendritic patches, respectively. In the majority of patches (three out of five CA3 and nine out of twelve CA1 dendritic patches), the time course of NMDA receptor-

Figure 10. Kinetics of AMPA receptor-mediated currents activated by glutamate

A, superimposed responses to 1, 10 and 100 ms pulses of 1 mM glutamate. B, the current deactivation in response to a 1 ms pulse was reasonably fitted by a single exponential function. A second exponential with an amplitude of opposite sign was used to fit the rising phase (grey line). C, the desensitizing response to a 100 ms pulse required a double exponential function to adequately describe the decay (grey line). Currents were obtained in the presence of 1 mM Mg^{2+} and 30 μM D-AP5, and in the absence of glycine. Each trace is an average of 8–14 sweeps (V_h was −50 mV). All data are from a CA3 dendritic patch taken at a distance of 47 μm from the border of the stratum lucidum.

A

10 pA

25 ms

1 ms, 1 mM glutamate

B

τ_{on} = 0·55 ms

τ_{off} = 2·2 ms

100 ms, 1 mM glutamate

C

τ_{on} = 0·37 ms

τ_{off1} = 4·9 ms (41%)

τ_{off2} = 19 ms (59%)
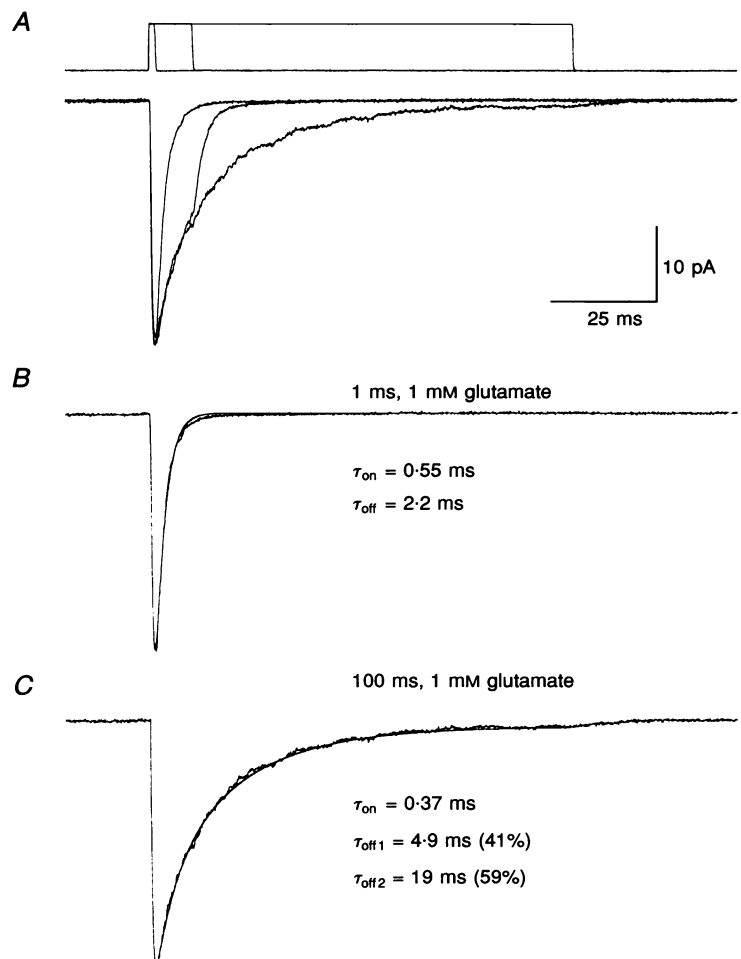
mediated current desensitization was reasonably fitted by a single exponential, which was significantly slower (t test, $P < 0.05$) in CA3 dendritic patches ($\sim$600 ms) than in CA1 dendritic patches ($\sim$450 ms; Table 1). In some patches, however, two exponentials provided a noticeably improved fit of the desensitization time course. An example of such a patch is shown in Fig. 11C. Patches in which two exponential fits of NMDA receptor-mediated current desensitization were reasonable yielded mean values of $\tau_1 = 169 \pm 37$ ms (48%) and $\tau_2 = 1306 \pm 281$ ms (52%) in four out of five CA3 dendritic patches and $\tau_1 = 218 \pm 27$ ms (61%) and $\tau_2 = 806 \pm 113$ ms (39%) in six out of twelve CA1 dendritic patches.

Mg^{2+} block of the NMDA receptor-mediated current

The voltage-dependent block of the NMDA component observed in dual-component responses in the presence of Mg^{2+} (Fig. 4) was studied in more detail using isolated NMDA receptor-mediated patch currents. Both the steady-state concentration–response relationship for Mg^{2+}-block of NMDA receptor channels and the kinetics of this block in response to voltage steps were studied.

Steady-state block by Mg^{2+}. The Mg^{2+} sensitivity of dendritic NMDA receptor channels evoked by 1 ms pulses of 1 mM glutamate was studied at −80 mV with varying concentrations of Mg^{2+} in both barrels of the application pipette. In CA3 dendritic patches, the concentration–response relationship for the block by Mg^{2+} could be satisfactorily described with an IC_{50} of 21 μM and a Hill coefficient of 0.85 (Fig. 12B). The full concentration–response relationship was not determined for CA1 patches but there was no noticeable difference from the Mg^{2+} block in CA3 patches at the concentrations tested (Fig. 12B). Micromolar Mg^{2+} concentrations reduced the amplitude of the NMDA receptor-mediated component in a manner that resembled the flickering open channel block (Fig. 12C) described by others (Ascher & Nowak, 1988).
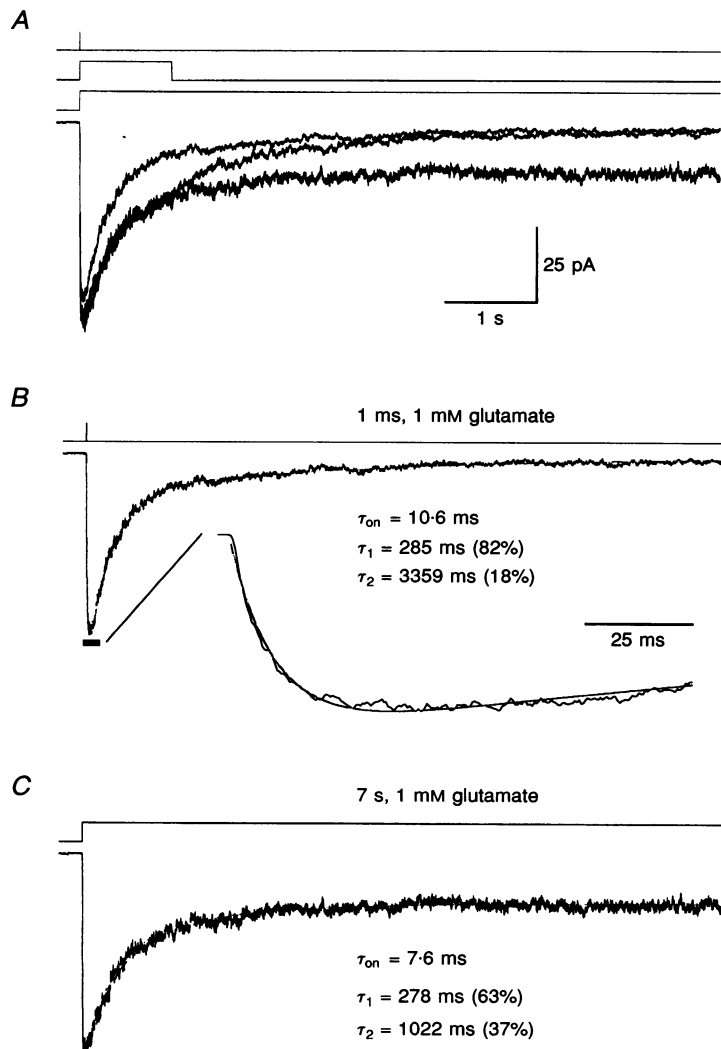
Figure 11. Kinetics of NMDA receptor-mediated currents activated by glutamate

A, superimposed responses to 1 ms, 1 s and 7 s pulses of 1 mM glutamate. B, the current response to 1 ms glutamate pulses was fitted by the sum of 3 exponentials consisting of a single exponential function describing the rising phase and a two-exponential decay. In the inset, the same trace is displayed on an expanded time scale for better resolution of the shape of the rising phase. C, desensitization of the current during 7 s glutamate pulses was best fitted with a two-exponential function (in addition to a single exponential for the rising phase). All data were obtained in solution containing 10 μM glycine, 5 μM CNQX and no added Mg^{2+}. Each trace is an average of 20–27 sweeps (V_h was −80 mV). All data are from a CA1 dendritic patch formed at a distance of 53 μm from the soma.

25 pA

1 s

B

1 ms, 1 mM glutamate

$\tau_{on} = 10.6$ ms
$\tau_1 = 285$ ms (82%)
$\tau_2 = 3359$ ms (18%)

25 ms

C

7 s, 1 mM glutamate

$\tau_{on} = 7.6$ ms
$\tau_1 = 278$ ms (63%)
$\tau_2 = 1022$ ms (37%)

A

Control

30 μM Mg²⁺

Recovery

5 pA

250 ms

B

IC₅₀ = 21 μM
n = 0·85

Normalized I_{NMDA}

[Mg²⁺] (μM)

C

Control

30 μM Mg²⁺

Recovery

5 pA

100 ms
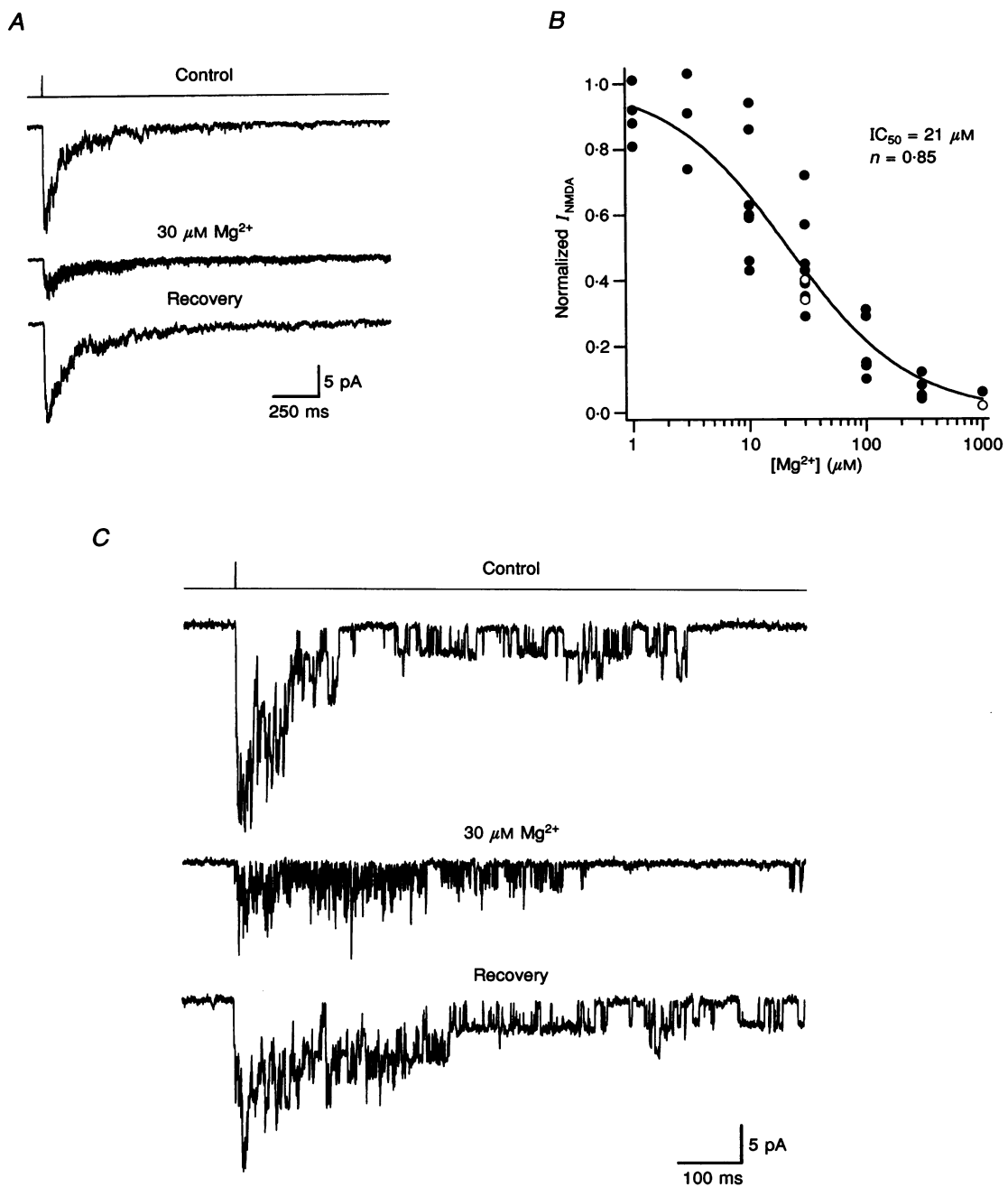
Figure 12. Block of NMDA receptor-mediated currents by external Mg²⁺

A, responses to 1 ms pulses of 1 mM glutamate before, during and after application of 30 μM Mg²⁺ (averages of 5–10 sweeps, V_h was −80 mV). *B*, concentration–response curve for the Mg²⁺ block of the current at −80 mV (CA3 dendritic patches, ●; CA1 dendritic patches, ○). Data points from the CA3 patches were fitted with the Hill equation:

$$I_{NMDA} = \frac{1}{1 + \left(\dfrac{[Mg^{2+}]}{IC_{50}}\right)^n}.$$

The fit yields an IC₅₀ of 21 μM and a Hill coefficient (*n*) of 0·85. All responses were obtained in external solution containing 10 μM glycine and 5 μM CNQX. Mg²⁺ was added to the solutions in both barrels of the application pipette. *C*, individual responses before, during and after addition of 30 μM Mg²⁺ ($V_h = -80$ mV). Data in *A* and *C* are from a CA3 dendritic patch taken at 37 μm from the border of the stratum lucidum.

Kinetics of block by Mg^{2+}. To determine how rapidly a change in current occurs due to induction or relief of Mg^{2+} block following a change in membrane potential, the voltage was stepped from a holding potential of +40 mV to a test potential of −80 mV for 50 ms at a time when the NMDA receptor-mediated current was near its peak (Fig. 13A). The current was turned off almost instantaneously by the jump to −80 mV (20–80% off time was 60 ± 8 μs, $n = 5$ dendritic
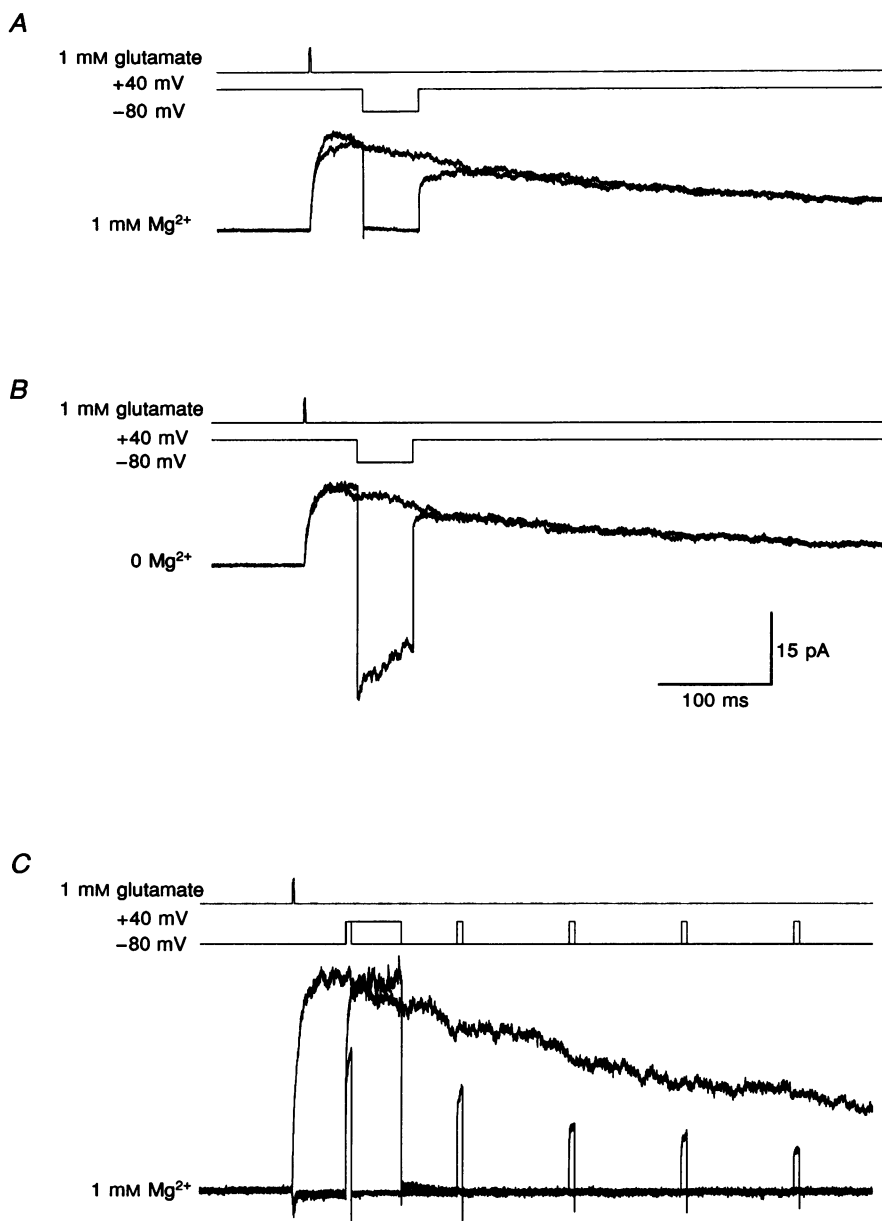
Figure 13. Rapid block and unblock of NMDA receptor-mediated currents by external Mg^{2+} in response to voltage steps

A, responses to 1 ms pulses of 1 mM glutamate at V_h = +40 mV and in the presence of 1 mM external Mg^{2+}. Currents evoked with and without a 50 ms voltage jump to −80 mV (leak and capacitive current subtracted) to turn off the current are superimposed. B, similar responses, but with no added Mg^{2+} so that the voltage jump from +40 to −80 mV rapidly reverses the direction of current flow. C, superimposed currents evoked by 1 ms pulses of 1 mM glutamate in the presence of 1 mM Mg^{2+} at +40 mV (without a step) and at −80 mV with either a single 50 ms step to +40 mV or five steps (5 ms each, 10 Hz) to +40 mV. All traces are averages of 4–30 sweeps in solution containing 10 μM glycine and 5 μM CNQX. In these experiments the current was filtered at 5 kHz and sampled at 20 kHz. Data in A and B are from a CA1 dendritic patch taken 63 μm from the soma and in C from a different CA1 dendritic patch taken 78 μm from the soma.

and 5 somatic patches). The recovery of the current at the end of the jump, however, had two components, a fast component (which predominated) and a second, slower component (Fig. 13A). This second, slow component of the

current recovery was also apparent (but smaller) in Mg^{2+}-free solution (Fig. 13B), suggesting that it may partly represent a slow component of Mg^{2+} unblock and partly a Mg^{2+}-independent process. An increase in open probability
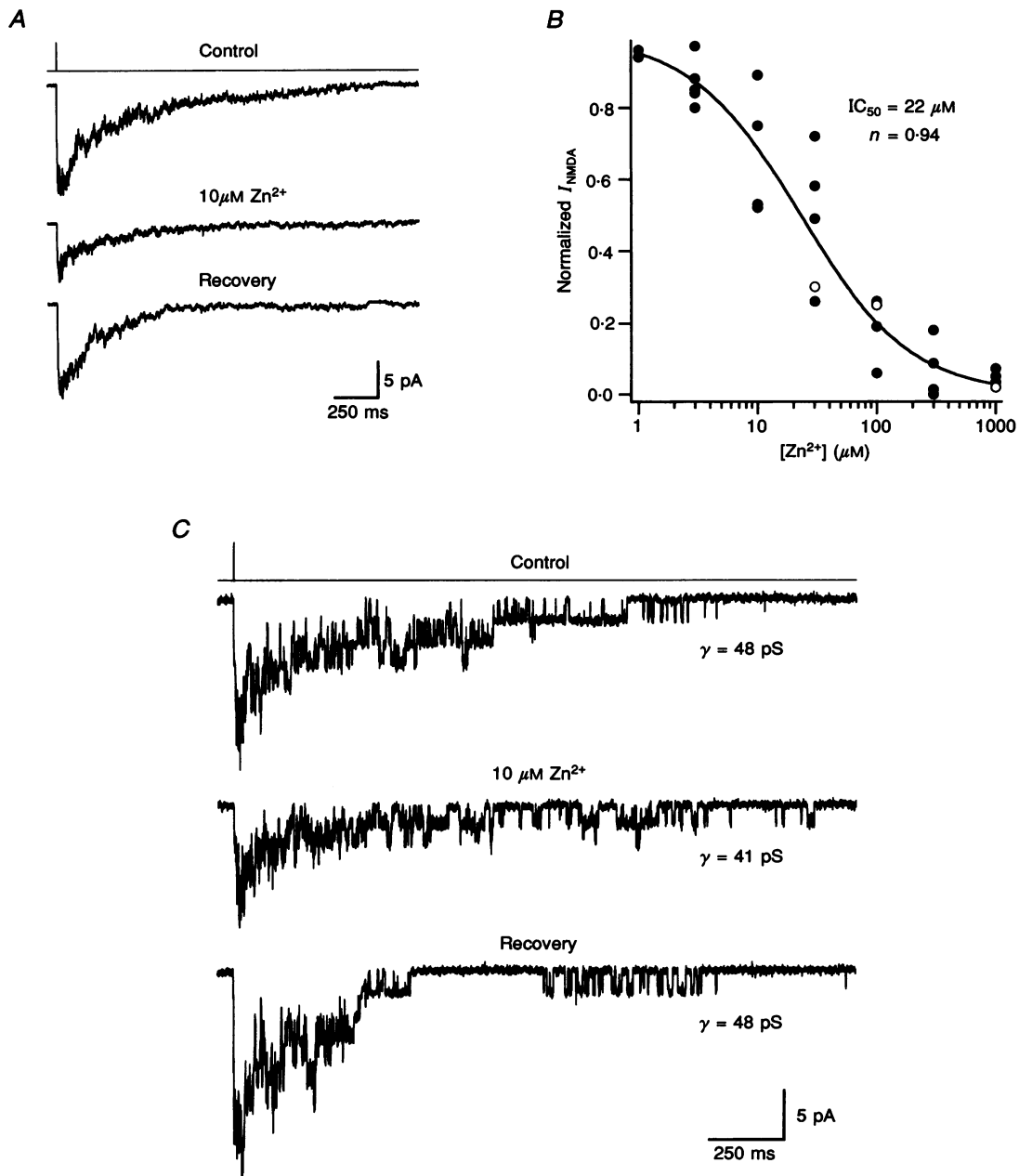
Figure 14. Block of NMDA receptor-mediated current by Zn^{2+}

A, responses to 1 ms pulses of 1 mM glutamate before, during and after application of 10 μM Zn^{2+} (averages of 10 sweeps, V_h was -50 mV). *B*, concentration–response curve for the Zn^{2+} block of the current at -50 mV (CA3 dendritic patches, ●; CA1 dendritic patches, ○). Data points from the CA3 patches were fitted with the Hill equation (see Fig. 12, legend) yielding an IC_{50} of 22 μM and n of 0.94. All responses were obtained in external solution containing 10 μM glycine, 5 μM CNQX, and no added Mg^{2+}. Zn^{2+} was added to the solutions in both barrels of the application pipette. *C*, individual responses before and after addition of 10 μM Zn^{2+} (V_h was -50 mV). The single-channel conductance (γ) of the main state is indicated. Data in *A* and *C* are from a CA3 dendritic patch taken at 30 μm from the border of the stratum lucidum.

of NMDA receptor channels at depolarized potentials, albeit with a much slower time course, has also been observed by others (Nowak & Wright, 1992).

Zn^{2+} block of the NMDA receptor-mediated current

Zn^{2+} ions are contained at high concentrations in MF boutons on CA3 pyramidal cells and there is evidence that they may be actively released during synaptic transmission (Assaf & Chung, 1984; Howell, Welch & Frederickson, 1984). Zn^{2+} is known to block NMDA receptor-mediated current (Legendre & Westbrook, 1990). We therefore investigated the effects of Zn^{2+} on NMDA receptors in dendritic membrane patches from CA3 pyramidal cells.

Steady-state block by Zn^{2+}. When included in the solutions in both barrels of the application pipette, micromolar concentrations of Zn^{2+} blocked NMDA receptor-mediated currents evoked by 1 ms pulses of 1 mM

glutamate. Unlike Mg^{2+}-block of the channel, block by Zn^{2+} was only weakly voltage-dependent; in the presence of 1 mM Zn^{2+}, block was complete at negative potentials and only small currents (about 20 % of control) could be evoked at positive potentials. Figure 14*A* and *C* shows the effects of 10 μM Zn^{2+} on average and individual NMDA responses, respectively. The IC_{50} for the NMDA component was 22 μM and the Hill coefficient was 0·94 (Fig. 14*B*).

Kinetics of block by Zn^{2+}. To determine how quickly Zn^{2+} is able to block the NMDA receptor channel, 1 mM Zn^{2+} was co-applied to the patch with 1 mM glutamate for 1 ms to mimic the corelease of Zn^{2+} with glutamate from synaptic vesicles. As shown in Fig. 15*A*, this results in only a small reduction of the peak current and slowing of the rising phase with respect to the response to glutamate alone, suggesting that Zn^{2+} does not prevent the binding of glutamate and subsequent opening of the channel. If,

A

1 mM glutamate
1 mM glutamate + 1 mM Zn^{2+}

Control

10 pA

50 ms

B

Control

C

Control
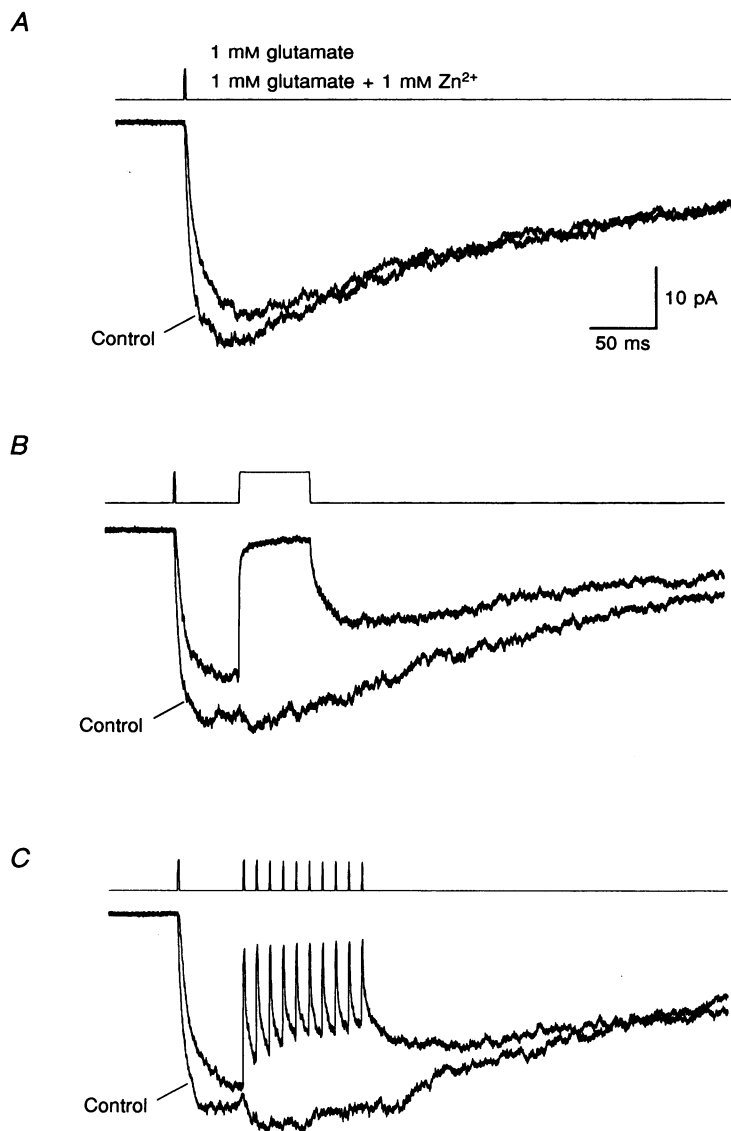
Figure 15. Kinetics of the block and unblock of NMDA receptor-mediated currents by Zn^{2+}

A, responses of a CA3 dendritic patch to 1 ms pulses of 1 mM glutamate both with and without 1 mM Zn^{2+} in the agonist solution. *B*, response of the same patch to a 1 ms pulse followed by a second, 50 ms glutamate pulse, with and without Zn^{2+} in the agonist solution. The first pulse activates the NMDA-type GluR channels, while the second pulse results in block of the current by Zn^{2+}. *C*, response of the same patch to a 1 ms glutamate pulse followed by 10 more 1 ms glutamate pulses at 100 Hz, with and without Zn^{2+} in the agonist solution. All data were obtained in solution containing 10 μM glycine and 5 μM CNQX, with no added Mg^{2+}. Each trace is an average of 22–27 sweeps (V_h was −50 mV). In these experiments the current was filtered at 5 kHz and sampled at 20 kHz. Data are from a CA3 dendritic patch taken at 39 μm from the border of the stratum lucidum.

however, a second, longer pulse (Fig. 15*B*) or a train of brief pulses (Fig. 15*C*) of Zn^{2+} plus glutamate was applied after the current had reached a peak, a strong block of the NMDA receptor-mediated current was observed. This block occurred quickly (20–80% decay time of 3.4 ± 1.5 ms, $n = 5$ CA3 dendritic patches), but was incomplete, perhaps because of the continued presence of glutamate during the Zn^{2+} pulse. Recovery from Zn^{2+} block was slower, occurring over a time period of about 50 ms.

DISCUSSION

The results presented provide a characterization of the functional properties of both AMPA and NMDA-type GluR channels in the apical dendrites of CA3 and CA1 pyramidal neurons of the hippocampus. No major differences were found between the properties of channels in somatic and dendritic patches. We have no direct evidence that outside-out dendritic patches contain synaptic receptors, but given the high density of spines on the dendrites of pyramidal neurons it seems likely that at least some of the channels in dendritic patches would be from subsynaptic membrane. Assuming that this is the case, our data suggest that synaptic and extrasynaptic GluR channels in hippocampal pyramidal neurons have similar properties.

Colocalization of AMPA and NMDA receptor channels in dendrites of CA3 and CA1 pyramidal neurons

Almost all patches isolated from both CA3 and CA1 dendrites as well as those from somata contained both AMPA and NMDA-type GluR channels. This indicates that segregation of AMPA and NMDA receptors in the dendrite is unlikely to occur, at least at the spatial resolution of the area of an outside-out patch (about 2 μm^2 for the pipettes used here; Sakmann & Neher, 1983). The ratio of peak NMDA to AMPA receptor-mediated current varied considerably from patch to patch. The range of this ratio was 0.03–0.62 and, on average, was about 0.20 in both CA3 and CA1 dendrites. This variability may reflect local predominance of either AMPA or NMDA receptor channels in different regions of dendritic membrane, perhaps even at individual synapses. Variability in the relative contributions of AMPA and NMDA-type GluR channels to EPSCs has also been shown (Bekkers & Stevens, 1989; Stern, Edwards & Sakmann, 1992).

Are there NMDA receptor channels at MF–CA3 synapses?

The demonstration of NMDA receptor channels in the dendrites of CA3 pyramidal neurons was surprising in view of the fact that binding studies had indicated that these dendrites are devoid of NMDA receptors in the region of MF termination (Monaghan, Holets, Toy & Cotman, 1983; Benke, Jones, Collingridge & Angelides, 1993). Further evidence for the existence of these receptors at MF synapses was recently provided by the demonstration of a component of the MF synaptic current in CA3 neurons that was mediated by NMDA receptor channels (Jonas *et al.* 1993).

However, determination of whether these channels are also present at MF–CA3 synapses in older animals and what role these channels might play in mediating synaptic plasticity at these synapses will require further investigation.

How many AMPA and NMDA receptor channels are located at a postsynaptic density opposite a release site?

Assuming that the present data from dendritic patches are representative for synaptic channels, it is possible to derive estimates of the number of functionally activated AMPA and NMDA receptor channels in the postsynaptic density of a hippocampal synapse. This estimate is based on the mean experimentally determined amplitude ratio of the NMDA to AMPA component of 0.2, the mean single-channel conductances of 10 pS for AMPA and 45 pS for NMDA receptors, the maximal open probabilities of 0.5–0.6 for AMPA and 0.05–0.3 for NMDA receptors (Jahr, 1992; Rosenmund, Clements & Westbrook, 1993; Hessler, Shirke & Malinow, 1993), and a mean quantal conductance change of 350 pS for the AMPA receptor-mediated EPSC (Jonas *et al.* 1993). Assuming that the glutamate pulse in the synaptic cleft is roughly equivalent to the 1 ms pulse of 1 mM glutamate used in the present experiments (Clements *et al.* 1992; see Jonas & Spruston, 1994 for discussion), the number of AMPA-type GluR channels open at the peak of an EPSC can be estimated as 35 and the number of available channels in the postsynaptic density would be 58–70. The mean NMDA to AMPA ratio estimated here implies that a quantal NMDA receptor-mediated EPSC would be 70 pS in the absence of Mg^{2+}, corresponding to the opening of only about two NMDA receptor channels at the peak. Based on estimates of $P_{o,max}$, this indicates that five to thirty NMDA receptor channels would be available in the postsynaptic density, similar to the number suggested for synapses on other neurons (Silver, Traynelis & Cull-Candy, 1992; Stern *et al.* 1992*b*).

The peak concentration of glutamate in the synaptic cleft may exceed 1 mM under some conditions (for review see Jonas & Spruston, 1994) and $P_{o,max}$ for AMPA receptor channels could then be as high as 0.8 (Jonas *et al.* 1993). Estimates of the number of available GluR channels opposite a release site would therefore have to be adjusted downward by about 20%. If, on the other hand, the glutamate concentration in the cleft is lower, these estimates would have to be adjusted substantially upwards.

Clues to the identity and subunit composition of dendritic non-NMDA receptor channels

Studies on recombinant GluR channels suggest that non-NMDA type responses may be mediated by either AMPA- or kainate-preferring receptors formed by subunits of the GluR-A to D and GluR-5 to 7 families, respectively (for review see Wisden & Seeburg, 1993). A number of observations support the conclusion that the fast component of the response evoked by glutamate in dendritic patches of hippocampal pyramidal neurons is

mediated almost exclusively by AMPA-preferring GluR channels. Firstly, the response to 1 mM AMPA was similar to the response to 1 mM glutamate, whereas the response to 1 mM kainate was much smaller. Secondly, desensitization is much less pronounced and the current response to a subsequent agonist pulse recovers more rapidly in response to kainate than in response to AMPA or glutamate. These desensitization properties differ markedly from those of kainate-preferring recombinant receptors (GluR-5 to 7), which desensitize strongly in response to kainate and recover very slowly from desensitization (Burnashev, 1993; Lerma, Paternain, Naranjo & Mellström, 1993). Thirdly, the responses to kainate we observe in dendritic patches are similar to those seen in cultured hippocampal neurons, which on the basis of block of the kainate-induced desensitization by cyclothiazide were inferred to be due to the action of kainate on AMPA-preferring GluR channels (Patneau et al. 1993).

Although we observed no responses in the dendrites of hippocampal pyramidal neurons resembling those mediated by kainate-preferring GluR channels, we cannot rule out the possibility that these receptors may contribute a small amount to the fast component of the glutamate response that was not detected with our experimental protocol. It is also possible that these receptors are expressed in subsets of hippocampal neurons (pyramidal or otherwise), as has been shown in cultured neonatal hippocampal neurons (Lerma et al. 1993).

The low Ca^{2+} permeability and close to linear $I-V$ relation of AMPA receptor channels in the dendrites of both CA3 and CA1 pyramidal neurons suggest that they include the edited form of the GluR-B subunit (Burnashev, 1993; Jonas, Racca, Sakmann, Seeburg & Monyer, 1994). Dendritic AMPA receptors were also characterized by desensitization time constants that suggest expression of the GluR-B subunit; other cells expressing low levels of the GluR-B subunit exhibit faster desensitization (Jonas et al. 1994).

Clues to the subunit composition of dendritic NMDA receptor channels

Functional properties of recombinant NMDA receptors coassembled from NR1 and NR2 subunits are largely determined by the NR2 subunit. Recombinant channels containing NR2A or NR2B subunits resemble the native channels with respect to high sensitivity to block by Mg^{2+} (maximum inward current at -20 mV with 1 mM external Mg^{2+}), whereas channels containing NR2C or NR2D are less sensitive to Mg^{2+} (maximum inward current at -40 mV; Monyer, Burnashev, Laurie, Sakmann & Seeburg, 1994). Furthermore, recombinant channels containing NR2A or NR2B subunits, like the native channels, show a high single-channel conductance (40–50 pS), whereas that of NR2C-containing channels is significantly lower (35 pS; Stern, Béhé, Schoepfer & Colquhoun, 1992b). Finally, recombinant channels containing NR2B, C or D subunits

resemble the native receptors with respect to slow deactivation (400–5000 ms), whereas deactivation of NR2A-containing channels is faster (100 ms; Monyer et al. 1994). Comparison of these properties with those of dendritic NMDA receptors in hippocampal pyramidal neurons suggests that the functional properties of the native channels may be dominated by the NR2B subunit.

Slow deactivation of NMDA receptor-mediated currents

NMDA receptor-mediated current in response to brief pulses of glutamate decayed very slowly in dendritic patches from CA3 and CA1 pyramidal cells, outlasting the 1 ms glutamate application by about 1000-fold. Deactivation was fitted with two time constants of ∼200 ms and 1–3 s, respectively, with the second time constant being slower in patches from CA1 than in those from CA3 neurons. Slow deactivation kinetics of NMDA receptor-mediated currents has been reported previously; the time constant values, however, were $\tau_1 < 100$ ms and $\tau_2 = 156$–600 ms (Lester et al. 1990; Edmonds & Colquhoun, 1992; Carmignoto & Vicini, 1992). The fast time constant reported here ($\tau_1 \approx 200$ ms) probably corresponds to a blend of the two time constants reported above, with the slower of the above time constants dominating because of the young age of the rats (Carmignoto & Vicini, 1992; Hestrin, 1992). The reason why a very slow component ($\tau_1 \approx 1$–3 s) has not been reported by others is unclear. One possibility is that the slow component was only detected here because very long sweeps (up to 7 s) were analysed. Another explanation might therefore be that the very slow component of NMDA receptor deactivation is a transient developmental state. Developmental regulation of NMDA receptor deactivation kinetics, similar to that reported in visual cortex and superior colliculus (Carmignoto & Vicini, 1992; Hestrin, 1992), and perhaps determined by a switch in subunit expression, could possibly control the appearance of the very slow component. In preliminary experiments, however, the slow component of the NMDA receptor-mediated current was also observed in patches isolated from CA1 dendrites of 21- to 28-day-old rats. Another possibility is that gating properties might change following patch formation, causing the slow component to disappear under certain recording conditions. It has been reported, for example, that the rate of desensitization can become faster with time following patch excision (Sather, Dieudonné, MacDonald & Ascher, 1992; Lester, Tong & Jahr, 1993). We did not observe any such changes. Finally, differences in the composition of the pipette solution may account for differences in the kinetics observed by various groups. The use of an ATP-regenerating system and GTP in the present experiments (the major difference) does not, however, account for the difference in kinetics, since omitting these components did not affect the time course of NMDA receptor-mediated currents (see Methods).

Comparison of currents evoked by brief glutamate pulses to EPSCs

Comparison of the time course of currents evoked by fast application of glutamate to outside-out patches with those evoked by synaptic stimulation requires consideration of the voltage- and space-clamp errors associated with whole-cell recordings from dendritic synapses (Spruston et al. 1993a). To evaluate how currents with the time courses determined here would be attenuated by dendritic filtering, conductances with this time course were used to simulate dual-component EPSCs at the soma and at three dendritic locations on spines attached to a cable representing the apical dendrites of a typical CA3 or CA1 hippocampal pyramidal neuron (Fig. 16A). The resulting currents (both for 0 and 1 mM external Mg^{2+}) measured with a voltage clamp at the soma are shown in Fig. 16B. As the synapse is placed at increasingly further distances from the soma, the time course of the AMPA receptor-mediated component is slowed, whereas the kinetics of the NMDA receptor-mediated component are hardly affected. Also, the peak amplitude of the AMPA receptor-mediated component decreases considerably, thus increasing the apparent NMDA to AMPA peak current ratio. For these reasons comparison of the kinetics of AMPA receptor-mediated EPSCs and the relative contributions of the two components should be limited to synapses that occur electrically close to the soma (Stern et al. 1992b; Silver et al. 1992; Jonas et al. 1993).

AMPA receptor-mediated component. In the hippocampus, MF synapses on CA3 pyramidal cells are located close to the soma and therefore EPSCs from these synapses are subject to relatively little distortion (Johnston & Brown, 1983; Jonas et al. 1993; Spruston et al. 1993a). The decay time constant of MF–CA3 EPSCs (as fast as 3 ms) is much closer to the deactivation time constant of AMPA receptor-mediated currents evoked by brief glutamate pulses than to the desensitization time constant evoked by longer glutamate pulses (see also Colquhoun et al. 1992). This finding suggests that the EPSC decay is largely determined by channel deactivation following rapid removal of transmitter from the synaptic cleft. This view is consistent with data from experiments on hippocampal neurons in culture using low-affinity competitive antagonists of the NMDA receptor, which suggest that the length of the glutamate concentration change occurring in the synaptic cleft is likely to be close to 1 ms (Clements et al. 1992). Nevertheless, desensitization could exert some influence on the kinetics of synaptic currents at some synapses under some conditions (for review, see Jonas & Spruston, 1994).

NMDA receptor-mediated component. NMDA receptor-mediated EPSCs with slow decays have been reported in many neuronal cell types (Lester et al. 1990; Keller, Konnerth & Yaari, 1991; Carmignoto & Vicini, 1992; Hestrin, 1992; Stern et al. 1992), although the slow

EPSC decay reported in these studies are not as slow as the decay of the patch currents we describe here. This could be a real difference between the kinetics of NMDA receptor channels at synapses and those in dendritic patches, or could simply be due to the difficulty in resolving small, slow components in whole-cell recordings of EPSCs. This will be an important issue to resolve, because the time course of the NMDA receptor-mediated EPSC may be critical for determining the interval over which the NMDA receptor channel may act as a coincidence detector of pre- and postsynaptic activity (see below). At physiological temperatures, the decay of the NMDA receptor-mediated current is likely to be faster than at room temperature; a Q_{10} of about 3 (Hestrin, Sah & Nicoll, 1990; Feldmeyer, Silver & Cull-Candy, 1993) would mean that the slowest component may be in the order of 300–800 ms at 37 °C, as opposed to 1–3 s at room temperature.

The data presented here are consistent with that of others, indicating that the slow decay of the NMDA receptor-mediated currents is due to channel kinetics rather than a prolonged presence of glutamate in the synaptic cleft (Hestrin et al. 1990b; Lester et al. 1990). At the single-channel level, a long latency from the binding of glutamate to the first opening of an NMDA receptor channel is one mechanism which could contribute to the slow decay of NMDA receptor-mediated currents (Edmonds & Colquhoun, 1992).

What are the relative contributions of AMPA and NMDA receptor channels during a dual-component EPSP?

With the data provided here, it is possible to estimate the relative contribution of AMPA and NMDA receptor channels to the EPSP. This can be done by considering the amount and time course of charge entry mediated by each component. It can be estimated by current integration that the NMDA component would contribute 97% in the absence of Mg^{2+} and 65% in the presence of Mg^{2+} to the total amount of charge entry (resting potential of −65 mV, peak NMDA to AMPA receptor-mediated conductance ratio of 0·2). The slow component of the NMDA receptor-mediated current decay is responsible for about 75% of the charge entry through these receptors. Although the AMPA component carries the minority of the total charge, it would produce a larger peak depolarization because of its larger peak current. The NMDA component would produce a smaller, more prolonged depolarization.

To estimate quantitatively the contribution of each component to the synaptic depolarization, it is necessary to perform simulations. Such simulations must include spines, as the synaptic potential there is much larger than in the dendrite or at the soma (Fig. 16C and D), which will affect the amount of Mg^{2+} block of NMDA receptor channels. The EPSP generated by a unitary dual-component conductance

change (black line) is compared with that of a pure AMPA receptor-mediated EPSP (in the presence of 1 mM Mg^{2+}, grey line). The peak EPSP is similar with and without the NMDA component, whereas the late phase differs substantially. The predominant effect of the NMDA component is to prolong the EPSP, thus increasing the time interval during which temporal summation of synaptic potential or Ca^{2+} influx into the dendritic spines could occur.
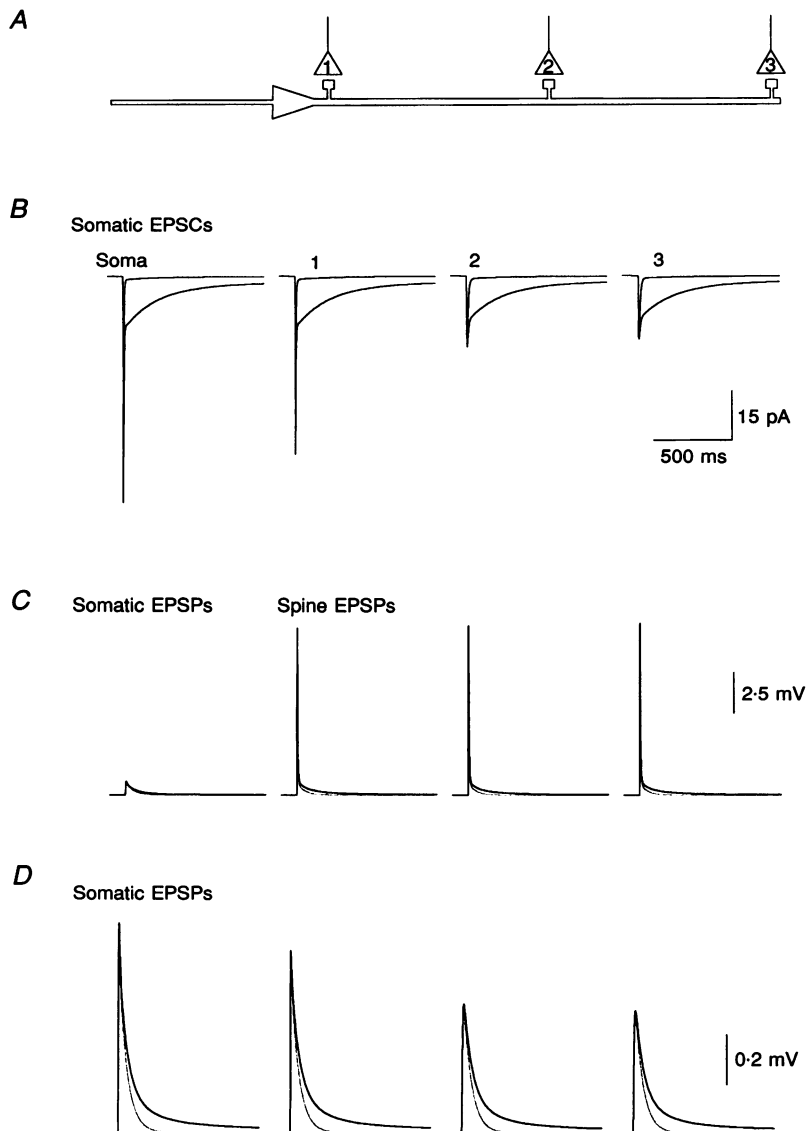
Figure 16. Dendritic filtering of AMPA and NMDA receptor-mediated EPSCs and EPSPs

A, schematic diagram of the simple pyramidal neuron model used for simulations. Soma and cable diameters are to scale, but cable lengths are 5% of actual lengths. Only one spine is shown at each synapse location (not to scale; see Methods). Synaptic inputs were simulated at the soma (no spines) or onto spines at each of positions 1, 2 and 3 corresponding to distances of 0, 310 and 648 μm from the soma, respectively. Details of the model are given in Methods. *B*, dual-component synaptic currents activated at the soma and positions 1, 2 and 3 and measured with a somatic voltage clamp at the resting potential (−65 mV) using a series resistance of 0·5 MΩ to simulate the best case of a low-resistance electrode with series resistance compensation. A peak AMPA-type GluR conductance of 350 pS (a 'quantal' conductance change) was simulated on each of 3 spine heads to simulate activation of synapses due to activity in a single axon (a 'unitary' EPSC; Jonas *et al.* 1993). Currents simulated for the cases of 0 and 1 mM external Mg^{2+} are shown. *C* and *D*, EPSPs at the synapse (*C*) and at the soma (*D*) are shown in response to activation of synapses at the soma or at positions 1, 2 and 3 (as described above). Both traces show the responses in the presence of 1 mM Mg^{2+}; black traces are with coactivation of NMDA and AMPA-type GluRs and grey traces with activation of AMPA-type GluRs alone.

How much Ca^{2+} enters through AMPA and NMDA receptor channels?

The data presented here can be used to estimate the amount of Ca^{2+} influx into a dendritic spine due to each quantal conductance change during a unitary synaptic event. From the time course of the AMPA and NMDA components and the Mg^{2+} sensitivity of the latter, a unitary EPSP under physiological conditions was simulated (Fig. 17A) at location 2 (see Fig. 16A). The relative Ca^{2+} permeability was used to estimate the Ca^{2+} influx through NMDA receptor channels during the EPSP. Because the permeability of AMPA receptor channels to Ca^{2+} was very low, Ca^{2+} entry through these channels was not considered. The Ca^{2+} influx through the NMDA receptor channels is shown, together with the total current through these channels, in Fig. 17B. These simulations reveal that during a quantal EPSP, about 72 000 Ca^{2+} ions enter the spine through NMDA receptor channels in a 6 s interval. About 42 000 of these Ca^{2+} ions enter during the first 1 s following onset of the current.

Because changes in membrane potential rapidly enhance or decrease Mg^{2+} block of NMDA receptor channels (Fig. 13), the effect of a series of backpropagating action potentials (Stuart & Sakmann, 1994) occurring during the decay phase of the EPSP was also modelled (Fig. 17). The action potentials (10 Hz) were elicited by AMPA-mediated EPSPs generated at location 1. In the first 1 s from the beginning of the EPSP, the train of backpropagating action potentials results in an additional 36% of Ca^{2+} entry into the spine through NMDA receptors. The enhanced Ca^{2+} influx caused by the additional depolarization is believed to endow the NMDA receptor with the ability to act as a coincidence detector of pre- and postsynaptic activity (Bliss & Collingridge, 1993). The slow decay of NMDA receptor-
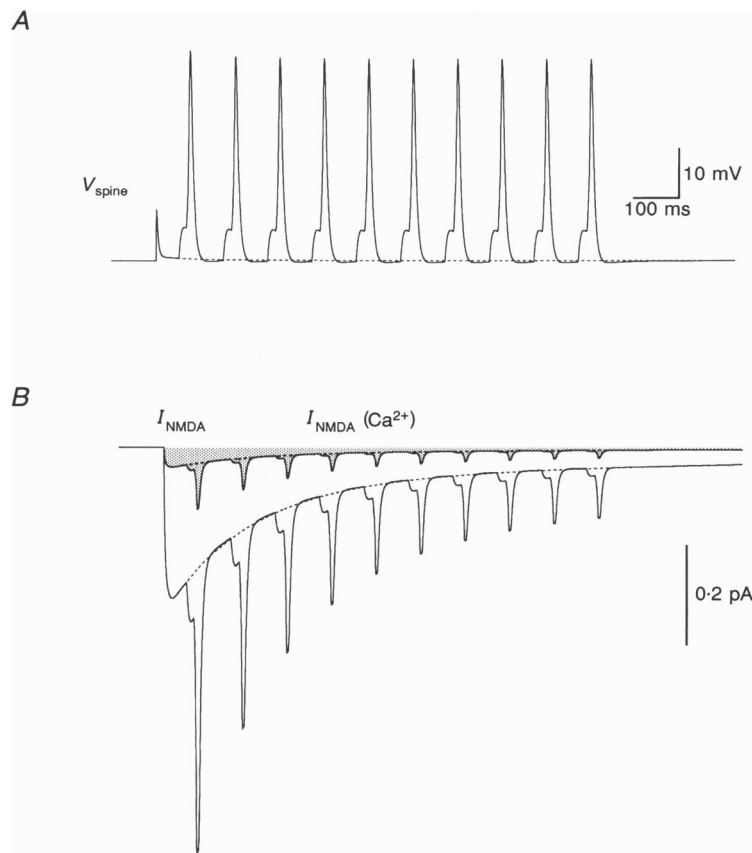
Figure 17. Physiological calcium inflow through NMDA receptor channels

A, the membrane potential at a single spine located at position 2 (Fig. 16A) is shown during a unitary conductance change as described in the text. Ten more larger conductance changes associated with activation of AMPA receptors alone at position 1 are simulated at 10 Hz, beginning 50 ms after the first event. Each large event in this synaptic tetanus corresponds to quantal events on 42 spines (equivalent to a composite EPSP comprised of 14 unitary events of ~1 nS each; Jonas *et al.* 1993) and evokes a spike at the soma which is then broadened and attenuated as it propagates back into the spine at position 2 (peak about −20 mV). B, current through the NMDA receptor channels in this single spine is shown along with the component of this current that is carried by Ca^{2+} (shaded). Dashed lines indicate the results of the simulation without the tetanus. Note that the action potential relieves the Mg^{2+} block of the NMDA receptor channels, causing an increase in Ca^{2+} entry into the spine.

mediated currents suggests that the time interval for coincidence detection could be in the order of seconds.

These simulations are simplified in a number of respects. First, the estimate of Ca^{2+} entry rests on the assumptions of the GHK formalism (see Methods). Combined electrophysiological and fluorescence measurements suggest that the the fraction of current through NMDA receptor channels carried by Ca^{2+} is slightly lower than that predicted by GHK (Schneggenburger *et al.* 1993; Burnashev, Zhou, Neher & Sakmann, 1995). The Ca^{2+} influx through NMDA receptor channels during the EPSP may thus be overestimated. Second, the presence of voltage-dependent Na^+ channels in the dendrite (Jaffe, Johnston, Lasser-Ross, Lisman, Miyakawa & Ross, 1992) is not considered. Na^+ channels may amplify the backpropagation of the action potential into the dendrite (Stuart & Sakmann, 1994) and thereby alter the effect of action potentials on Ca^{2+} influx. Similarly, the presence of voltage-activated Ca^{2+} and K^+ channels in the dendrite or spine could affect the spine voltage and the degree of NMDA receptor channel block.

It is important to point out that dendritic action potentials also cause Ca^{2+} entry through voltage-activated Ca^{2+} channels. This route of Ca^{2+} influx appears to be quite large relative to entry through NMDA receptor channels (Miyakawa *et al.* 1992). Understanding the relative roles of these two distinct paths for dendritic Ca^{2+} entry will require future study. One might speculate that a spatially localized Ca^{2+} inflow into dendritic spines at which prior activation of NMDA receptor channels had occurred could be functionally distinct from a generalized increase in internal Ca^{2+} as would be mediated by voltage-activated Ca^{2+} channels.

Modulation of NMDA receptor-mediated EPSCs by Zn^{2+}

Block of the NMDA receptor channel by Zn^{2+} may endow this receptor channel with the ability to behave differently under conditions of low- and high-frequency presynaptic activity at synapses where Zn^{2+} is co-released with glutamate. This may be particularly important at MF synapses on CA3 pyramidal neurons, where Zn^{2+} is contained in and released from a subset of presynaptic vesicles (Assaf & Chung, 1984; Howell, Welch & Frederickson, 1984; Pérez-Clausell & Danscher, 1985). The data presented here suggest that Zn^{2+} released from presynaptic boutons would be more effective at blocking the NMDA receptor channel under conditions of high-frequency presynaptic activity. As seen in Fig. 15*B* and *C*, however, block by Zn^{2+} during repetitive stimulation is likely to be less effective than the block produced by prolonged elevation of Zn^{2+}, which might occur if the diffusion of Zn^{2+} from the synaptic cleft were somehow hindered. It has been estimated that during convulsive activity the local extracellular concentration of Zn^{2+} could be as high as 300 μM (Assaf & Chung, 1984; Howell *et al.* 1984), which would be high enough to almost completely block the NMDA receptor-mediated component of the EPSC at MF–CA3 synapses. The induction of long-term potentiation at MF–CA3 synapses is thought to be insensitive to NMDA receptor channel blockers (Johnston, Williams, Jaffe & Gray, 1992). It is tempting to speculate that block of NMDA-type GluRs by Zn^{2+} released during tetanic

synaptic stimulation might reduce or eliminate the ability of Ca^{2+} influx through NMDA-type GluR channels to induce long-term potentiation at these synapses and that other mechanisms for inducing long-term potentiation have evolved (Johnston *et al.* 1992; Bliss & Collingridge, 1993).

ASCHER, P. & NOWAK, L. (1988). The role of divalent cations in the *N*-methyl-D-aspartate responses of mouse central neurones in culture. *Journal of Physiology* **399**, 247–266.

ASSAF, S. Y. & CHUNG, S.-H. (1984). Release of endogenous Zn^{2+} from brain tissue during activity. *Nature* **308**, 734–736.

BEKKERS, J. M. & STEVENS, C. F. (1989). NMDA and non-NMDA receptors are co-localized at individual excitatory synapses in cultured rat hippocampus. *Nature* **341**, 230–233.

BENKE, T. A., JONES, O. T., COLLINGRIDGE, G. L. & ANGELIDES, K. J. (1993). *N*-methyl-D-aspartate receptors are clustered and immobilized on dendrites of living cortical neurons. *Proceedings of the National Academy of Sciences of the USA* **90**, 7819–7823.

BLISS, T. V. P. & COLLINGRIDGE, G. L. (1993). A synaptic model of memory: long-term potentiation in the hippocampus. *Nature* **361**, 31–39.

BURNASHEV, N. (1993). Recombinant ionotropic glutamate receptors: functional distinctions imparted by different subunits. *Cellular Physiology and Biochemistry* **3**, 318–331.

BURNASHEV, N., ZHOU, Z., NEHER, E. & SAKMANN, B. (1995). Fractional calcium currents through recombinant GluR channels of the NMDA, AMPA and kainate receptor subtypes. *Journal of Physiology* (in the Press).

CARMIGNOTO, G. & VICINI, S. (1992). Activity-dependent decrease in NMDA receptor responses during development of the visual cortex. *Science* **258**, 1007–1011.

CLEMENTS, J. D., LESTER, R. A. J., TONG, G., JAHR, C. E. & WESTBROOK, G. L. (1992). The time course of glutamate in the synaptic cleft. *Science* **258**, 1498–1501.

COLQUHOUN, D., JONAS, P. & SAKMANN, B. (1992). Action of brief pulses of glutamate on AMPA/kainate receptors in patches from different neurones of rat hippocampal slices. *Journal of Physiology* **458**, 261–287.

CULL-CANDY, S. G., HOWE, J. R. & OGDEN, D. C. (1988). Noise and single channels activated by excitatory amino acids in rat cerebellar granule neurones. *Journal of Physiology* **400**, 189–222.

EDMONDS, B. & COLQUHOUN, D. (1992). Rapid decay of averaged single-channel NMDA receptor activations recorded at low agonist concentration. *Proceedings of the Royal Society* B **250**, 279–286.

FELDMEYER, D., SILVER, R. A. & CULL-CANDY, S. G. (1993). Temperature dependence of EPSC time course at the rat mossy fibre–granule cell synapse in thin cerebellar slices. *Journal of Physiology* **459**, 481*P*.

FORSYTHE, I. D. & WESTBROOK, G. L. (1988). Slow excitatory postsynaptic currents mediated by *N*-methyl-D-aspartate receptors on cultured mouse central neurones. *Journal of Physiology* **396**, 515–533.

GIBB, A. J. & COLQUHOUN, D. (1992). Activation of *N*-methyl-D-aspartate receptors by L-glutamate in cells dissociated from adult rat hippocampus. *Journal of Physiology* **456**, 143–179.

HESSLER, N. A., SHIRKE, A. M. & MALINOW, R. (1993). The probability of transmitter release at a mammalian central synapse. *Nature* **366**, 569–572.

HESTRIN, S. (1992). Developmental regulation of NMDA receptor-mediated synaptic currents at a central synapse. *Nature* **357**, 686–689.

HESTRIN, S. (1993). Different glutamate receptor channels mediate fast excitatory synaptic currents in inhibitory and excitatory cortical neurons. *Neuron* **11**, 1083–1091.

HESTRIN, S., NICOLL, R. A., PERKEL, D. J. & SAH, P. (1990*a*). Analysis of excitatory synaptic action in pyramidal cells using whole-cell recording from rat hippocampal slices. *Journal of Physiology* **422**, 203–225.

HESTRIN, S., SAH, P. & NICOLL, R. A. (1990*b*). Mechanisms generating the time course of dual component excitatory synaptic currents recorded in hippocampal slices. *Neuron* **5**, 247–253.

HINES, M. (1993). NEURON – a program for simulation of nerve equations. In *Neural Systems: Analysis and Modeling*, ed. EECKMAN, F., pp. 127–136. Kluwer Academic Publishers, Norwell, MA, USA.

HOWELL, G. A., WELCH, M. G. & FREDERICKSON, C. J. (1984). Stimulation-induced uptake and release of zinc in hippocampal slices. *Nature* **308**, 736–738.

IINO, M., OZAWA, S. & TSUZUKI, K. (1990). Permeation of calcium through excitatory amino acid receptor channels in cultured rat hippocampal neurones. *Journal of Physiology* **424**, 151–165.

JAFFE, D. B., JOHNSTON, D., LASSER-ROSS, N., LISMAN, J. E., MIYAKAWA, H. & ROSS, W. N. (1992). The spread of Na$^+$ spikes determines the pattern of dendritic Ca^{2+} entry into hippocampal neurons. *Nature* **357**, 244–246.

JAHR, C. E. (1992). High probability opening of NMDA receptor channels by L-glutamate. *Science* **255**, 470–472.

JAHR, C. E. & STEVENS, C. F. (1987). Glutamate activates multiple single channel conductances in hippocampal neurons. *Nature* **325**, 522–525.

JAHR, C. E. & STEVENS, C. F. (1993). Calcium permeability of the N-methyl-D-aspartate receptor channel in hippocampal neurons in culture. *Proceedings of the National Academy of Sciences of the USA* **90**, 11573–11577.

JOHNSTON, D. & BROWN, T. H. (1983). Interpretation of voltage-clamp measurements in hippocampal neurons. *Journal of Neurophysiology* **50**, 464–486.

JOHNSTON, D., WILLIAMS, S., JAFFE, D. & GRAY, R. (1992). NMDA-receptor-independent long-term potentiation. *Annual Review of Physiology* **54**, 489–505.

JONAS, P., MAJOR, G. & SAKMANN, B. (1993). Quantal components of unitary EPSCs at the mossy fibre synapses on CA3 pyramidal cells of rat hippocampus. *Journal of Physiology* **472**, 615–663.

JONAS, P., RACCA, C., SAKMANN, B., SEEBURG, P. H. & MONYER, H. (1994). Differences in Ca^{2+} permeability of AMPA-type glutamate receptor channels in neocortical neurons caused by differential GluR-B subunit expression. *Neuron* **12**, 1281–1289.

JONAS, P. & SPRUSTON, N. (1994). Mechanisms shaping glutamate-mediated excitatory postsynaptic currents in the CNS. *Current Opinion in Neurobiology* **4**, 366–372.

KELLER, B. U., KONNERTH, A. & YAARI, Y. (1991). Patch clamp analysis of excitatory synaptic currents in granule cells of rat hippocampus. *Journal of Physiology* **435**, 275–293.

LEGENDRE, P. & WESTBROOK, G. L. (1990). The inhibition of single N-methyl-D-aspartate-activated channels by zinc ions on cultured rat neurones. *Journal of Physiology* **429**, 429–449.

LERMA, J., PATERNAIN, A. V., NARANJO, J. R. & MELLSTRÖM, B. (1993). Functional kainate-selective glutamate receptors in cultured hippocampal neurons. *Proceedings of the National Academy of Sciences of the USA* **90**, 11688–11692.

LESTER, R. A. J., CLEMENTS, J. D., WESTBROOK, G. L. & JAHR, C. E. (1990). Channel kinetics determine the time course of NMDA receptor-mediated synaptic currents. *Nature* **346**, 565–567.

LESTER, R. A. J., TONG, G. & JAHR, C. E. (1993) Interactions between the glycine and glutamate binding sites of the NMDA receptor. *Journal of Neuroscience* **13**, 1088–1096.

McBAIN, C. & DINGELDINE, R. (1992). Dual-component miniature excitatory synaptic currents in rat hippocampal CA3 pyramidal neurons. *Journal of Neurophysiology* **68**, 16–27.

MIYAKAWA, H., ROSS, W. N., JAFFE, D., CALLAWAY, J. C., LASSER-ROSS, N., LISMAN, J. E. & JOHNSTON, D. (1992). Synaptically activated increases in Ca^{2+} concentration in hippocampal CA1 pyramidal cells are primarily due to voltage-gated Ca^{2+} channels. *Neuron* **9**, 1163–1173.

MONAGHAN, D. T., HOLETS, V. R., TOY, D. W. & COTMAN, C. W. (1983). Anatomical distributions of four pharmacologically distinct ^{3}H-L-glutamate binding sites. *Nature* **306**, 176–179.

MONYER, H., BURNASHEV, N., LAURIE, D. J., SAKMANN, B. & SEEBURG, P. H. (1994). Developmental and regional expression in the rat brain and functional properties of four NMDA receptors. *Neuron* **12**, 529–540.

NOWAK, L., BREGESTOVSKI, P., ASCHER, P., HERBERT, A. & PROCHIANTZ, A. (1984). Magnesium gates glutamate-activated channels in mouse central neurones. *Nature* **307**, 462–465.

NOWAK, L. M. & WRIGHT, J. M. (1992). Slow voltage-dependent changes in channel open-state probability underlie hysteresis of NMDA responses in Mg^{2+}-free solutions. *Neuron* **8**, 181–187.

PATNEAU, D. K., VYKLICKY, L. JR & MAYER, M. (1993). Hippocampal neurons exhibit cyclothiazide-sensitive rapidly desensitizing responses to kainate. *Journal of Neuroscience* **13**, 3496–3509.

PÉREZ-CLAUSELL, J. & DANSCHER, G. (1985). Intravesicular localization of zinc in rat telencephalic boutons. A histochemical study. *Brain Research* **337**, 91–98.

ROSENMUND, C., CLEMENTS, J. D. & WESTBROOK, G. L. (1993). Nonuniform probability of glutamate release at a hippocampal synapse. *Science* **262**, 754–757.

SAKMANN, B. & NEHER, E. (1983). Geometric parameters of pipettes and membrane patches. In *Single Channel Recording*, ed. SAKMANN, B. & NEHER, E., pp. 37–51. Plenum Press, New York.

SATHER, W., DIEUDONNÉ, S., MACDONALD, J. F. & ASCHER, P. (1992). Activation and desensitization of N-methyl-D-aspartate receptors in nucleated outside-out patches from mouse neurones. *Journal of Physiology* **450**, 643–672.

SCHNEGGENBURGER, R., ZHOU, Z., KONNERTH, A. & NEHER, E. (1993). Fractional contribution of calcium to the cation current through glutamate receptor channels. *Neuron* **11**, 133–143.

SIGWORTH, F. J. (1980). The variance of sodium current fluctuations at the node of Ranvier. *Journal of Physiology* **307**, 97–129.

SILVER, R. A., TRAYNELIS, S. F. & CULL-CANDY, S. G. (1992). Rapid-time-course miniature and evoked excitatory currents at cerebellar synapses *in situ*. *Nature* **355**, 163–166.

Spruston, N., Jaffe, D. B., Williams, S. H. & Johnston, D. (1993a). Voltage- and space-clamp errors associated with the measurement of electrotonically remote synaptic events. *Journal of Neurophysiology* **70**, 781–802.

Spruston, N., Jonas, P. & Sakmann, B. (1993b). Properties of AMPA and NMDA channels in the apical dendrites of CA3 pyramidal neurons. *Society for Neuroscience Abstracts* **19**, 624.

Stern, P., Béhé, P., Schoepfer, R. & Colquhoun, D. (1992a). Single-channel conductances of NMDA receptors expressed from cloned cDNAs: comparison with native receptors. *Proceedings of the Royal Society* B **250**, 271–277.

Stern, P., Edwards, F. A. & Sakmann, B. (1992b). Fast and slow components of unitary EPSCs on stellate cells elicited by focal stimulation in slices of rat visual cortex. *Journal of Physiology* **449**, 247–278.

Stuart, G. J., Dodt, H.-U. & Sakmann, B. (1993). Patch-clamp recordings from the soma and dendrites of neurons in brain slices using infrared video microscopy. *Pflügers Archiv* **423**, 511–518.

Stuart, G. J. & Sakmann, B. (1994). Active propagation of somatic action potentials into neocortical pyramidal cell dendrites. *Nature* **367**, 69–72.

Traynelis, S. F., Silver, R. A. & Cull-Candy, S. G. (1993). Estimated conductance of glutamate receptor channels activated during EPSCs at the cerebellar mossy fibre–granule cell synapse. *Neuron* **11**, 279–289.

Wisden, W. & Seeburg, P. H. (1993). Mammalian ionotropic glutamate receptors. *Current Opinion in Neurobiology* **3**, 291–298.

Woodhull, A. M. (1973). Ionic blockage of sodium channels in nerve. *Journal of General Physiology* **61**, 687–708.